JBC Papers in Press. Published on May 3, 2016 as Manuscript M115.670521
The latest version is at http://www.jbc.org/cgi/doi/10.1074/jbc.M115.670521

Tumour necrosis factor-stimulated gene (TSG)6-mediated Interactions with the Inter–alpha-Inhibitor Heavy Chain 5 facilitate TGFβ1-dependent Fibroblast to Myofibroblast Differentiation

John Martin, Adam Midgley, Soma Meran, Emma Woods, Timothy Bowen, Aled O Phillips* and Robert Steadman*

From the Department of Nephrology, Institute of Molecular and Experimental Medicine, Cardiff University School of Medicine and Cardiff Institute of Tissue Engineering & Repair, Heath Park, Cardiff CF14 4XN, UK

**These authors made an equal contribution to this work*

Running title*: IαI heavy chain 5 and myofibroblast differentiation.*

To whom correspondence should be addressed: Robert Steadman, Department of Nephrology, Institute of Molecular and Experimental Medicine, Cardiff University School of Medicine and Cardiff Institute of Tissue Engineering & Repair, Heath Park, Cardiff CF14 4XN, UK Tel: 44-2920-748390, Fax: 44-2920-748470, Email: steadmanr@cf.ac.uk

Keywords: Fibroblast, myofibroblast, hyaluronan, tumor necrosis factor stimulated gene-6, transforming growth factor β1

ABSTRACT

Fibroblasts are central to wound healing and fibrosis through Transforming Growth Factor-β1 (TGF-β1)-triggered differentiation into contractile, α-smooth muscle actin (α-sma)-positive myofibroblasts. This is mediated by accumulation of a pericellular matrix of hyaluronan (HA) and the HA-dependent co-localisation of CD44 with the Epidermal Growth Factor Receptor (EGFR). Interactions of HA with hyaladherins, such as Inter-alpha-Inhibitor (IaI) and Tumour Necrosis Factor-stimulated gene-6 (TSG-6) are also essential for differentiation. This study investigated the mechanisms involved. TSG-6 and α-sma had different kinetics of induction by TGF-β1, with TSG-6 peaking before α-sma. siCD44 or EGFR inhibition prevented differentiation but had no effect on TSG-6 expression. TSG-6 was essential for differentiation, and mAb A38 (preventing IαI heavy chain [HC] transfer), HA-oligosaccharides, Cobalt, or siBikunin prevented TSG-6 activity, preventing differentiation. A38 also prevented the EGFR/CD44 association. This suggested that TSG-6/IαIHC interaction was necessary for the effect of TSG-6 and that HC-stabilisation of HA initiated the CD44/EGF-R association. The newly-described HC5 was shown to be the principal HC expressed and its cell surface expression was prevented by siRNA inhibition of TSG-6 or Bikunin. HC5 was released by hyaluronidase treatment, confirming its association with cell surface HA. Finally, HC5 knock down by siRNA confirmed its role in myofibroblast differentiation. The current study describes a novel mechanism linking the TSG-6 transfer of the newly-described HC5 to the HA-dependent control of cell phenotype. The interaction of HC5 with cell surface HA was essential for TGF-β1-dependent differentiation of fibroblasts to myofibroblasts, highlighting its importance as a novel potential therapeutic target.

The fibroblast is the most abundant cell type in normal connective tissues. It plays a central role in the synthesis, degradation and remodelling of extracellular matrix both in health and in disease. At sites of tissue damage and in the context of wound healing, activated fibroblasts, termed myofibroblasts, with a contractile phenotype, characterised by the expression of the smooth muscle isoform of α-actin (α-sma), are essential for the synthesis of a collagen-rich scar, providing the force for wound contraction (1). During a healing response, myofibroblasts are a transient cell population (2). Myofibroblasts are also the major effectors of fibrosis, their persistent presence has been established as the best marker of numerous types of progressive organ dysfunction such as that seen in chronic renal failure of various aetiologies (3, 4, 5, 6, 7), liver disease (8) and pulmonary fibrosis (9).

The cytokine Transforming Growth Factor Beta-1 (TGF-β1) is a well recognised mediator of progressive tissue fibrosis and *in vitro* and *in vivo* evidence suggest that it is the primary driving force in fibroblast-myofibroblast phenotypic activation (10, 11). The sequence of events leading up to this transformation is being increasingly characterised at a molecular level in an attempt to understand and eventually control this process.

We have previously demonstrated that TGF-β1-mediated phenotypic activation is dependent on an increase in the synthesis of the extracellular matrix polysaccharide hyaluronan (HA) (12, 13, 14). TGF-β1, through stimulation of EGF and subsequent activation of EGFR-associated ERK-MAP kinase activity stimulates HA synthesis. This increased HA synthesis is associated with the formation of an organised pericellular HA coat which subsequently orchestrates assembly of a CD44/EGFR receptor complex on the cell surface. Activation of ERK signalling downstream of this complex subsequently leads to a re-organisation of the actin cytoskeleton.

The secreted product of Tumor Necrosis Factor-stimulated Gene 6 (TSG-6) is important in the formation and remodelling of HA-rich pericellular coats and matrices (14, 15, 16,). It is involved in the formation of TSG-6 cross-linked HA networks (17) and may also stabilise the HA matrix either by binding directly as a hyaladherin, or through facilitating the covalent transfer of heavy chains of inter-alpha-inhibitor (IαI) onto HA to form a HC/HA complex (18, 19). Thus in the TGF-β1-triggered generation of the myofibroblast phenotype, we proposed that TSG-6 may play an important part in forming the HA/CD44/EGFR complex, which then signals to induce ERK activation.

The mechanism of heavy chain (HC) transfer has been elucidated by Rugg et al (19). TSG-6 forms an intermediate species with one of the two heavy chains from the IαI complex, which consists of the light chain bikunin and its chrondroitin sulphate (CS) chain which is bound to 2 heavy chains. Classically, three HC's have been described. HC1 and HC2 are known to occur bound to CS to form IaI, while HC3 is thought to bind CS/bikunin as a single chain forming an assembly known as pre-αI. Previous work (20) has shown that TSG-6 is capable of transferring not only HC2 but also HC1 and HC3 from IαI (or pre-αI) onto HA, but that the presence of HC2 appeared to be necessary for this enzymatic action of TSG-6 to take place.

There is a fourth HC (HC4) about which less is known. It does not have the conserved cleavage site of HC1-3 that allows them to link with Bikunin. It does, however, bind to and block the polymerization of actin, resulting in inhibition of neutrophil phagocytosis and chemotaxis (21). The more recently described HC5 has not yet been fully characterised, nor shown to complex with CS to form IαI (or pre IαI). It does, however, possess the necessary binding sites to enable it to do so (22) (Fig 1) The existence of HC6 was recently identified in Genebank from a report of 2003 (23) but no protein product has yet been described.

In the current manuscript we have examined the role of TSG-6 following TGF-β1 stimulation and highlighted HC transfer activity as being key to form a HA matrix which is anchored by CD44 leading to a CD44:EGF-R signalling complex. This activity was specifically dependent on HC5. We demonstrate for the first time that HC5 has a major mechanistic role to play in the phenotypic activation of fibroblasts.

MATERIALS AND METHODS

Materials.

All reagents were from Sigma-Aldrich (Poole, UK) unless otherwise stated.. ERK (MEK) inhibitor PD98059 and EGF-R inhibitor AG1478 were purchased from Calbiochem (Darmstadt, Germany). They were prepared as stock solutions of 5 mg/ml and 3 mg/ml respectively. Oligo HA (10 units; i.e. 10 monosaccharides) (purchased from Hyalose, Oklahoma City; HYA-OLIGO10EF-1) and a hexasaccharide control (Iduron UK) were prepared at a concentration of 1 mg/ml, and was added to give a final concentration of 50 μg/ml on the cells 2 h prior to stimulation with TGFβ. Cobalt Chloride was stored at a concentration of 500 mM in PBS. All inhibitors were diluted immediately before use and added to the cell cultures at the times given in the legends before addition of TGF-β1. Anti IaI heavy chain 5 antibody ab107846 and anti IaI heavy chain 2 antibody ab118257 together with the loading control anti GAPDH antibody ab9485 were purchased from Abcam (Cambridge UK).

Cell Culture

Primary human lung fibroblasts (AG02262; NIA Ageing Cell Respiratory Corriel Institute, NJ, USA) were cultured in Dulbecco's modified Eagle's medium (DMEM) and F-12 medium containing 2 mM L-glutamine, 100 units/ml penicillin, and 100 µg/ml streptomycin supplemented with 10% fetal calf serum (FCS) (Biologic Industries Ltd., Cumbernauld, UK). The cells were maintained at 37°C in a humidified incubator in an atmosphere of 5% CO_2, and fresh growth medium was added to the cells every 3-4 days until confluence. Cells were growth arrested in serum-free medium for 48 hours before use in experiments, and all experiments were performed under serum-free conditions unless otherwise stated. For the induction of differentiation cells were exposed to a single treatment of TGF-β1 at the concentrations indicated for times up to 72 hrs as in previous studies (12-14).

Reverse Transcription (RT) and Real-Time Quantitative Polymerase Chain Reaction (QPCR-RT)

Cells were grown in 35 mm dishes and washed with phosphate-buffered saline (PBS), pH 7.3, prior to lysis with tri-reagent and RNA purification according to the manufacturer's protocol. RNA was precipitated with isopropanol and washed with 70% ethanol before being dried and resuspended in water. The concentration of RNA was determined by the absorbance at 260 nm. Reverse transcription was performed on 1mg of RNA, using random primers to initiate cDNA synthesis with High Capacity cDNA reverse transcription kits, according to the manufacturer's protocol (Applied Biosystems, Cheshire, UK). As a negative control, RT was performed with sterile H_2O replacing the RNA sample. qPCR was carried out using a 7900HT Fast Real Time PCR System (Applied Biosystems, Cheshire, UK). cDNA was diluted 4 fold and 4 ml (equivalent to 0.05 mg of the original RNA) was amplified in a final volume of 20 ml containing 10 ml Taqman master mix (Applied Biosystems), 5 ml H_2O and 1 ml specific primer.

The following primers were purchased from Applied Biosystems:-

α-SMA primer ACTA2 Cat No 4331182 Hs00426835_g1

TSG-6 primer TNFAIP6 Cat No Hs00200180_m1

rRNA was used as the internal control for all samples, and the results presented as the RQ calculated by the delta delta CT method using the equation: $2^{-[\Delta CT(1)-\Delta CT(2)]}$ (where ΔCT(1) is the mean ΔCT calculated for the experimental samples and ΔCT(2) is the mean ΔCT calculated for the control samples (Applied Biosystems, Cheshire, UK).

Heavy chain amplification was carried out by qPCR of the cDNA with specific primers to each IaI heavy chain using SYBR Green (Applied Biosystems).
In selected experiments mRNA copy number was determined by amplifying each heavy chain by conventional PCR and calculating the number of molecules present in the purified amplified product. Serial dilutions from 300,000 to 30 copies were prepared for each heavy chain and the amplified qPCR signal of the experimental samples read off the standard curves produced.
All oligonucleotide primers were purchased from Invitrogen (Paisley U.K.)
The Inter-alpha Trypsin Inhibitor Heavy chain (ITIH) qPCR primers used were: -

ITIH1 F TCCATGGAGAACAACGGACG

ITIH1 R GGGGGTACTGCAAATCCACA

ITIH2 F GCCATTTCGATGGTGTTCCG

ITIH2 R TTCTCTGCTGTGCTACCGTG

ITIH3 F CCTTTCGGCTGCTTGGGAAA

ITIH3 R GACGGCTCTCATGGTGACAA

ITIH4 F AGTCACCAAACCCGATGACC

ITIH4 R GCTCCAGCTGAGTGGACATT

ITIH5 F ACTGTCGCTGGAGAACTGTG

ITIH5 R CGGGGTCCTGATTTCATCGT

ITIH6 F CATTGCATGGAAGCCGATGG

ITIH6 R GGCTCCTGGTTGCTATGGTT

The FnEDR qPCR primers used were: -

FnEDR F GCTCAGAATCCAAGCGGAGA

FnEDR R CCAGTCCTTTAGGGCGATCA

Inhibition by siRNA

All siRNA was purchased from Life Technologies Ltd, Paisley.

SiRNA (TSG-6)	Cat.# M16704/s14263
SiRNA (Bikunin)	Cat. # 4392420/s1311
SiRNA (CD44)	Cat.#AM16704/114068
SiRNA (ITIH5)	Cat.# 4392420/s37361
SiRNA (ITIH2)	Cat. # 439 20/s7604
SiRNA (Smad 2)	Cat.# M16704/107875
SiRNA (Smad 3)	Cat.# M16704/115717

Silencer® Negative Control No. 2 siRNA Cat. #AM4613

Cells to be transfected were deprived of serum for 4 h before the addition of the siRNA. Briefly, Lipofectamine 2000 (Invitrogen) was diluted 1/50 in Optimem (Gibco 31085) and allowed to stand for 5 min. This was then added to a 333 nM dilution of the siRNA prepared immediately before use from a 100 μM stock. The mixture was left at room temp for 30 min to allow the Lipofectamine:siRNA complexes to form, then 200 μl of this preparation was added to 800 μl of serum-free antibiotic-free medium on the cells to give a final concentration of 33 nM and the transfection allowed to take place overnight. Control cells were transfected with scrambled siRNA. The following day the appropriate stimuli were added to the cells as described, without removing the siRNA complexes and the incubation continued for a further 72h (unless otherwise indicated) before isolating RNA. Typical knockdown ranges using these siRNA's were SiTSG6, 51% to 60%; SiBikunin, 78% to 89%; SiCD44, 53% to 67%; SiHC5, 89% to 98%; HC2, 90% to 99%..

SDSPAGE and Western Blotting

Cells were cultured for 72h under the designated conditions before total cell protein was extracted in 100 μl lysis buffer as previously described (24). Protein concentration was determined by the Bradford protein assay and 30 μg of each sample was boiled with reducing buffer for 10 minutes before being subjected to SDS-PAGE on a 7.5% acrylamide gel. Western blotting with rabbit anti-IαI HC5 primary antibody (Abcam, cat) was performed by standard methods to detect the presence of HC5. Detection was performed with a specific anti rabbit HRP conjugated antibody (Abcam Cat. 970510 and ECL reagent. Equal loading was confirmed by the use of anti GAPDH antibody (Abcam Cat 9485).

Immunocytochemistry

Cells were growth arrested before incubation with TGFβ1 (10ng/ml) or serum-free medium alone in the presence or absence of anti-TSG-6 Ab A38 (Santa Cruz: sc-65886) at 50 μg/ml. After 72h cells were fixed with 4% paraformaldehyde at room temperature for 15min. Fixed cells were stained for EGF-R (Abcam GR01 1:30), visualised using AlexaFluor 488) and CD44 (Ab A020 1:200) (Merck Millipore), visualised with AlexaFluor 555). The images were merged to demonstrate the co-localisation of CD44 and EGF-R.

The unpaired two-tailed Student's *t*-test was used to identify statistical significance. Data were analysed using the software GraphPad Prism version 4.0a (GraphPad Software Inc., La Jolla, CA, USA) and *P≤ 0.05 and **P≤ 0.01 were considered significant.

RESULTS

In association between induction of TSG-6 and phenotypic activation of fibroblasts

TSG-6 has been shown to be essential for the TGFβ1-dependent phenotypic activation of fibroblasts and renal epithelial cells (14, 16, 25). In order to determine the temporal relationship between TSG-6 expression and induction of the myofibroblast phenotype, growth arrested fibroblasts were stimulated with TGF-β1 (10 ng/ml) and mRNA was extracted at times up to 72 hours. Addition of TGF-β1, led to a time-dependent induction of TSG-6 that was significant at 3 h, reached a maximum at 8 h and was sustained to 72 h. In contrast the induction of the phenotypic markers, alpha-sma and the EDA isoform of fibronectin (fnEDA), was slower, becoming significant at 24 h and continuing to increase up to 72 h. There was no significant change in the levels of Bikunin over this time-course (Fig 2). These

results suggest but do not confirm, in themselves, a temporal separation between TSG-6 up-regulation and induction of phenotypic activation.

To investigate whether the induction of TSG-6 and alpha-sma were both triggered by a CD44-dependent mechanism, siRNA was used to knockdown CD44 expression. This resulted in >50% inhibition of CD44 protein expression (Fig3A), which was associated with a 60% inhibition of alpha-sma mRNA (Fig 3B) as reported previously (14, 23, 26). Knocking down CD44, however, had no inhibitory effect on TSG-6 expression (Fig 3C). The change of phenotype in response to TGF-β1 is also, however, dependent on EGF-R activation (14). Following inhibition of EGF-R activity by AG 1478, α-sma induction was inhibited by >99% (Fig 3D), TSG-6 expression, however, was unaffected (Fig 3E). Phosphorylation of ERK 1&2 is downstream from the EGFR-CD44 interaction. To confirm that TSG-6 was not induced as a result of this signalling pathway, ERK activation by MEK was inhibited using PD98059. This inhibited α-sma induction by approximately 60% but TSG-6 was again unaffected (Fig 3 F&G). Taken together these results indicate that TSG-6 was not induced by the same series of activation events as those leading to phenotypic change and, together with our previous work (14, 16, 24) that it may, therefore lie upstream of formation of the EGF-R:CD44 complex.

Induction of TSG-6 is Smad dependent

Although induction of HA and HA synthase is dependent on TGF-ß1 activation of ERK and subsequently the EGF-R, classical TGF-ß1 signalling is initiated when the ligand induces assembly of a heteromeric complex of type II and type I receptors. The RII kinase then phosphorylates RI on a conserved glycine-serine rich domain. This activates the RI kinase, which subsequently recognises and phosphorylates members of the intracellular receptor regulated Smads (Smad2 and Smad3). Smad signalling through the activation of this classical pathway has previously been implicated in phenotypic activation of fibroblasts, through the use of chemical inhibition of the ALK5 receptor (26). The role of Smad signalling was examined by gene silencing of either Smad 2 or Smad3 using siRNA. The siRNA to Smad2 caused between 60% and 70% knockdown of Smad2 in these cells with the siSmad 3 giving between 50% and 60% knockdown of Smad3 (Fig 4). Smad gene knockdown inhibited TGF-ß1 dependent induction of TSG-6 and phenotypic activation, reflected by an inhibition of TGF-ß1 induction of the myofibroblast marker, alpha-sma (Fig 4 A and B). These data therefore suggest that both Smad dependent and independent pathways are required for phenotypic activation, with the Smad pathway alone leading to induction of TSG-6, which is distinct from the signalling pathway leading to HA synthesis and HA-dependent signalling.

The mechanism of TSG-6 action in phenotypic activation of fibroblasts

TSG-6 binds directly to HA through its link module. In addition, by a separate mechanism, TSG-6 also supports the covalent transfer of heavy chains (HCs) of the IαI family members to HA, both of which roles are likely to stabilise HA matrices. The IαI family exists as a distinct assembly of one bikunin chain with one or more unique heavy (HC) chains designated HC1, HC2, HC3, HC5 and HC6 (HC4 does not bind bikunin). Covalent transfer of heavy chains to TSG-6 requires the bikunin component of IαI and is irreversibly inhibited by Cobalt (19). Gene silencing of Bikunin significantly inhibited TGF-β1-dependent phenotypic activation of fibroblasts, as did the presence of 1 mM cobalt (Fig 5 A&C). Neither intervention influenced TGF-β1-dependent induction of TSG-6 (Fig 5 B&D). TSG-6 function has been previously shown to be inhibited by the rat anti-human TSG-6 monoclonal antibody A38, which blocks HC binding to TSG-6 (27) and inhibits the formation of TSG-6-HC complexes *in vitro* (28). Similarly, HA decasaccharides (Oligo HA) irreversibly compete with HC binding to HA, preventing HA assembly, while hexasaccharides are ineffective. Stimulation of fibroblasts with TGFβ1 in the presence of either Oligo HA, to prevent HA binding by HC (Fig 5 E&F), or of the A38 antibody, at a concentration previously demonstrated to inhibit TSG-6 activity *in vitro* (16) (Fig 5 G&H), inhibited phenotypic activation, without affecting TGF-β1 induction of TSG-6. These data suggest that the function of TSG-6 that is critical for phenotypic activation is covalent transfer of heavy chains of IαI to HA which subsequently forms an organised and stable HA matrix.

To confirm that TSG-6-dependent covalent heavy chain transfer onto HA was required to drive receptor co-localisation, fibroblasts were stimulated with TGFβ1 in the presence of the A38 antibody. After 72 hours cells were dual-labelled for CD44

(red) and EGF-R (green). The results demonstrate an increased association of CD44 and EGF-R (yellow) following TGF-β1 stimulation, which was inhibited by the presence of the anti-TSG-6 A38 antibody (Figure 6). These results are therefore consistent with TSG-6 mediated heavy chain stabilisation of the HA matrix driving CD44 – EGF-R co-localisation. The phenotypic change triggered by TGF-β1 is therefore dependent on the induction of TSG-6, which, through catalytic transfer of IaI HCs, orchestrates HA-dependent CD44-EGFR interactions and triggers downstream ERK signalling pathways.

The heavy chain 5 of inter-alpha-inhibitor is highly expressed by fibroblasts and is linked to myofibroblast formation.

In order to investigate the role of each of the heavy chains of IαI in phenotypic activation, qPCR was performed for each of the chains HC1 to HC6. All of the chains were expressed and repeated analysis to obtain absolute values for the copy numbers of each transcript showed that HC5 was consistently very highly expressed compared to minimal expression of either HC1 or HC2 (Fig 7A). HC1 and HC2 proteins were not detected on the cells either by immunocytochemistry or Western blotting of cell lysates (not shown). In contrast, HC5 protein expression was examined by Western blot of cell lysates and, while low in unstimulated cells, it was strongly induced by TGF-β1 treatment (Fig 7B). Following treatment of the fibroblasts with a low concentration of trypsin before lysis, HC5 became undetectable by Western blot, suggesting that the majority of the HC5 detected in the original lysates was extracellular and associated with the cell surface. Cell surface expression of HC5 was confirmed by immunocytochemistry in both untreated and TGF-β1-treated cells (Fig 7C) and was reduced by exposure of the cells to Streptomyces hyaluronidase

The data generated above all suggest the importance of interactions between TSG-6 and HC5 for controlling the change in phenotype of the fibroblasts. To investigate whether these proteins could be found in higher molecular weight complexes, supernatants from the cells incubated in serum-free medium or treated with TGF-β1 were probed for TSG-6, HC5 and Bikunin. TGF-β1 induced the expression of all three proteins in the cell supernatants (Fig 8 A) and they were all also present as components of higher molecular weight complexes. Treatment of supernatants with Chondroitinase ABC resulted in a reduction of HC5-containing complexes (molecular weight 100-130 kDa, approximately), without affecting the non-complexed HC5 band, confirming that HC5 is present in IαI complexes with Bikunin.

To confirm the importance of TSG-6 in making HC5 an integral part of the pericellular HA matrix, cells were treated with siTSG-6 then lysed and Western blot performed for HC5 (Fig 9A). There was a marked reduction in HC5 levels similar to the effect of direct knockdown of HC5 (Fig 9b), when compared to treatment with scrambled control or siHC2 (Fig 9C). Treatment with siBikunin also markedly reduced HC5 levels, suggesting that HC5 must be part of an IaI or pre-aI complex to be functional (Fig 9D). To confirm that active TSG-6 was needed for HC5 incorporation into the pericellular matrix, cells were treated with, oligo HA (Fig 9E), Cobalt (Fig 9F) or mab A38 (Fig 9G). All reduced HC5 protein levels markedly. To examine the mechanisms holding HC5 at the cell surface, cells were treated with hyaluronidase (Fig 9H) or with si CD44 (Fig 9I). Both treatments reduced HC5 levels detected by Western blot, demonstrating that an association with HA and the presence of this HA binding receptor were essential for anchoring HC5 at the cell surface.

HC5 knockdown was used to investigate the functional significance of the HC5 associations at the cell surface described above. Knockdown of HC5 was >95% (Fig 10A) and resulted in a reduction in TGF-β1-simulated alpha-sma expression of >50% (Fig 10B). There was no effect of knockdown on TSG-6 expression (Fig 10C), confirming the independence of the HA-dependent differentiation pathway and the TSG-6 induction pathway.

DISCUSSION

Hyaluronan is a ubiquitous connective tissue glycosaminoglycan that, *in vivo,* is present as a high-molecular mass component of the extracellular matrix. In addition to its role in providing cellular support, it is known that under normal circumstances, HA regulates cell-cell adhesion, migration, proliferation, differentiation and the movement of interstitial fluid and macromolecules

(reviewed in 29) As a result it is likely to be an important contributor to and a regulator of, tissue remodelling. Our primary interest is understanding the pathogenesis of progressive fibrosis particularly in the context of renal disease. In a study of patients with biopsy proven diabetic nephropathy we have previously demonstrated an association between the deposition of hyaluronan and the degree of renal fibrosis, which is a known predictor of clinical outcome (30). This led us to examine the role of HA in regulation of fibroblast phenotype.

We have demonstrated that the phenotypic effects of TGF-β1 in fibroblasts are orchestrated by its stimulation of HA synthesis and accumulation in a pericellular coat (12, 13, 14, 26). The formation of this coat and the resulting change in cell phenotype is shown in this study to be dependent on the induction and activity of the hyaladherin, TSG-6. Inhibition of TSG-6 expression or its HC-transfer ability strongly inhibited the phenotypic change of fibroblasts to myofibroblasts. Many cell types assemble HA in an organized pericellular coat *in vitro*, in which the HA is anchored to the cell-surface by CD44 (16, 31, 32, 33, 34 35). Our recent studies in proximal tubular epithelial cells have investigated the roles of the IαI family of hyaladherin proteins, together with TSG-6 and the HA-binding proteoglycans bikunin and versican in the macro-molecular assembly of HA by PTC (16, 25, 35, 36). The results demonstrated that the TSG-6-mediated formation of IαI HC-HA complexes was critical for the formation of a pericellular HA matrix.

The data included in this manuscript suggest that it is the HC:HA catalytic activity of TSG-6 that is the key for the phenotypic activation of fibroblasts. Both TSG-6:HC formation and the subsequent HC transfer onto HA are metal ion-dependent. Previous studies have demonstrated the reaction to be dependent on either Mg^{2+} or Mn^{2+} and to be inhibited by Co^{2+} (19). Inhibition of TGF-β1 dependent phenotypic activation without any effect on the induction of TSG-6 itself is therefore consistent with a HC transfer function of TSG-6 orchestrating matrix assembly and phenotypic activation. This is further supported by the inhibition of phenotypic activation by the stimulation of fibroblasts with TGF-β1 in the presence of the rat anti human monoclonal antibody A38. This antibody has previously been demonstrated to block HA binding to TSG-6 (27), and inhibit the formation of TSG-6:HCs complexes *in vitro* (28). The transfer of HC, requires an intact IaI protein, as evidenced by female mice lacking the bikunin gene, which express the HCs but are unable to assemble IaI/preaI and which do not form cumulus-oocyte HC/HA complexes (37, 38). Our data using bikunin RNA silencing to inhibit the phenotypic activation of fibroblasts is therefore again compatible with the HC transfer catalytic activity of TSG-6 being a key component of acquisition of the myofibroblast phenotype.

TSG-6 mediated organisation of the HA matrix has been reported previously to alter the interaction of HA with its principle cell surface receptor CD44. For example in solution, TSG-6/HA complexes enhance or induce binding of HA to cell surface CD44 (39). It is well established that an organised pericellular HA coat is anchored to cell surface CD44 (34). We have previously demonstrated that phenotypic activation of fibroblasts requires HA driven formation of CD44-EGF-R complexes, and this together with the data in this manuscript suggests that TSG-6-dependent HC:HA interactions lead to the formation of a pericellular HA matrix which facilitates CD44 re-localisation within the cell membrane. This receptor complex then activates a downstream signalling cascade which is responsible for re-organisation of the actin cytoskeleton (24).

While this study demonstrates the importance of TSG-6-dependent HC:HA interactions, rather than the well-described HC1-3 involvement seen in epithelial cells, the essential and necessary HC for triggering HA transfer and the phenotypic change in fibroblasts was HC5. Its importance was further emphasised by the fact that in cell supernatants HC5 was only found in high molecular weight complexes and not as a monomer. In addition, while the mRNA levels of HC5 decrease following TGF-β1 treatment, the cell-associated protein levels increase, suggesting that the most important regulation of HC5 is not transcriptional but post-transcriptional through its incorporation into the HA pericellular matrix of the cell.

HC5 plays a role in tumour suppression with dysregulated or reduced expression of HC5 directly linked to tumour development (22, 40, 41) and its overexpression leading to suppression of cell migration and colony spreading (42). A recent study also found that HC5 was the major heavy chain expressed in skin, predominantly due to its production by dermal fibroblasts (43). The authors

conclude that HC5 may play an important role in inflammation through its interaction with HA. To our knowledge this report of Huth et al is the first description of a role for HC5 outside the area of tumourigenesis and metastasis and adds to the important role for HC5 described in our current study.

In summary, much has been previously published on the anti-inflammatory role of the hyaladherin TSG-6. The data in this manuscript provide evidence that it is also involved in driving a pro-fibrotic response through its catalytic transfer of HC5 to HA and that the mechanisms regulating TSG-6 and HA synthesis during this pro-fibrotic, TGF-β1-dependent process are distinct.

FOOTNOTES

Abbreviations Used:

TGF-β1	Transforming Growth Factor-β1
α-sma	α-smooth-muscle actin
EGFR	Epidermal Growth Factor Receptor
IαI	Inter-alpha-Inhibitor
TSG-6	Tumour Necrosis Factor-stimulated gene-6
HC	IαI heavy chain
HA	Hyaluronan
CS	Chrondroitin sulphate
4 MU	4-methyl-umbelliferone
DMSO	diMethylsulphoxide
FCS	Fetal calf serum
RT	Reverse Transcription

QPCR-RT	Real-Time Quantitative Polymerase Chain Reaction
PBS	Phosphate-buffered saline
SDSPAGE	Sodium dodecyl sulfate polyacrylamide gel electrophoresis
FnEDR	EDA isoform of fibronectin
Oligo HA(6 or 10)	Hyaluronan oligosaccharides (6 or 10 monosaccharide units)

ACKNOWLEDGEMENTS

The authors would like to thank Kidney Wales Foundation for their financial support of this work.

Conflict of Interest

The authors declare that they have no conflicts of interest with the contents of this article.

Author Contributions

JM performed the majority of the experimental work for this manuscript with experimental and technical advice from SM, TB, EW and AM. AP and RS jointly supervised the work. RS & JM wrote the manuscript with contributions from AP.

REFERENCES:

1) Gabbiani, G. (2003). The myofibroblast in wound healing and fibrocontractive diseases. The Journal of Pathology, 200, 500-503.

2) Tomasek, J. J., Gabbiani, G., Hinz, B., Chaponnier, C. & Brown, R. A. (2002). Myofibroblasts and mechano-regulation of connective tissue remodelling. Nat Rev Mol Cell Biol, 3, 349-363.

3) Eddy, A. A. (2005). Progression in Chronic Kidney Disease. Advances in Chronic Kidney Disease, 12, 353-365.

4) Essawy, M., Soylemezoglu, O., Muchaneta-Kubara, E. C., Shortland, J., Brown, C. B. & El Nahas, A. M. (1997). Myofibroblasts and the progression of diabetic nephropathy. Nephrology Dialysis Transplantation, 12, 43-50.

5) Goumenos, D., Tsomi, K., Iatrou, C., Oldroyd, S., Sungur, A., Papaioannides, D., Moustakas, G., Ziroyannis, P., Mountokalakis, T. & El Nahas, A. (1998). Myofibroblasts and the progression of crescentic glomerulonephritis. Nephrol. Dial. Transplant., 13, 1652-1661.

6) Goumenos, D. S., Brown, C. B., Shortland, J. & El Nahas, A. M. (1994). Myofibroblasts, predictors of progression of mesangial IgA nephropathy? Nephrology Dialysis Transplantation, 9, 1418-1425.

7) Roberts, I. S., Burrows, C., Shanks, J. H., Venning, M. & McWilliam, L. J. (1997). Interstitial myofibroblasts: predictors of progression in membranous nephropathy. J Clin Pathol, 50, 123-127.

8) Desmouliere, A., Darby, I. A. & Gabbiani, G. (2003). Normal and pathologic soft tissue remodeling: the role of the myofibroblast, with special emphasis on liver and kidney fibrosis. Laboratory Investigation, 83, 1689-1707.

9) Kuhn, C. & McDonald, J. A. (1991). The role of the myofibroblast in idiopathic pulmonary fibrosis. The American Journal of Pathology, 138, 1257-1265.

10) Evans, R. A., Tian, Y. C., Steadman, R. & Phillips, A. O. (2003). TGF-beta1-mediated fibroblast-myofibroblast terminal differentiation-the role of Smad proteins. Experimental Cell Research, 282, 90-100.

11) Vaughan, M. B., Howard, E. W. & Tomasek, J. J. (2000). Transforming growth factor ß1 promotes the morphological and functional differentiation of the myofibroblast. Exp Cell Res, 257, 180-189.

12) Meran, S., Thomas, D., Stephens, P., Martin, J., Bowen, T., Phillips, A. & Steadman, R. (2007). Involvement of Hyaluronan in Regulation of Fibroblast Phenotype. J. Biol. Chem., 282, 25687-25697.

13) Simpson, R., Meran, S., Thomas, D., Stephens, P., Bowen, T., Steadman, R. & Phillips, A. (2009). Age related changes in peri-cellular hyaluronan organisation leads to impaired dermal fibroblast to myofibroblast differentiation. The American Journal of Pathology, 175:1915-1928.

14) Simpson, R. M. L., Wells, A., Thomas, D., Stephens, P., Steadman, R. & A.O., P. (2010). Ageing Fibroblasts resist phenotypic maturation due to impaired Hyaluronan-dependent CD44/EGF receptor signalling. The American Journal of Pathology, 176: 1215-1228.

15) Fulop, C., Szanto, S., Mukhopadhyay, D., Bardos, T., Kamath, R. V., Rugg, M. S., Day, A. J., Salustri, A., Hascall, V. C., Glant, T. T. & Mikecz, K. (2003). Impaired cumulus mucification and female sterility in tumor necrosis factor-induced protein-6 deficient mice. Development, 130, 2253-2261.

16) Selbi, W., Day, A. J., Rugg, M. S., Fülöp, C., de la Motte, C. A., Bowen, T., Hascall, V. C. & Phillips, A. O. (2006a). Over-expression of hyaluronan synthase 2 alters hyaluronan distribution and function in proximal tubular epithelial cells. The Journal of the American Society of Nephrology, 17, 1553-1567.

17) Baranova, N. S., Nileback, E., Haller, F. M., Briggs, D. C., Svedhem, S., Day, A. J. & Richter, R. P. (2011). The inflammation-associated protein TSG-6 cross-links hyaluronan via hyaluronan-induced TSG-6 oligomers. J Biol Chem, 286, 25675-25686.

18) Blom, A. M., Mörgelin, M., Öyen, M., Jarvet, J. & Fries, E. (1999). Structural characterisation of inter-a-inhibitor. The Journal of Biological Chemistry, 274, 298-304.

19) Rugg, M. S., Willis, A. C., Mukhopadhyay, D., Hascall, V. C., Fries, E., Fulop, C., Milner, C. M. & Day, A. J. (2005). Characterization of complexes formed between TSG-6 and inter-alpha -inhibitor that act as intermediates in the covalent transfer of heavy chains on to hyaluronan. The Journal of Biological Chemistry, 280, 25674-25686.

20) Sanggaard, K. W., Sonne-Schmidt, C. S., Krogager, T. P., Lorentzen, K. A., Wisniewski, H.-G., Thogersen, I. B. & Enghild, J. J. (2008). The Transfer of Heavy Chains from Bikunin Proteins to Hyaluronan Requires Both TSG-6 and HC2. J. Biol. Chem., 283, 18530-18537.

21) Choi-Miura NH, Takahashi K, Yoda M, Saito K, Hori M, Ozaki H, Mazda T, Tomita M. (2000) The novel acute phase protein, IHRP, inhibits actin polymerization and phagocytosis of polymorphonuclear cells. Inflamm Res. 49(6):305-10.

22) Himmelfarb M, Klopocki E, Grube S, Staub E, Klaman I, Hinzmann B, Kristiansen G, Rosenthal A, Dürst M, Dahl E. ITIH5, a novel member of the inter-alpha-trypsin inhibitor heavy chain family is downregulated in breast cancer. (2004) Cancer Lett. 10;204(1):69-77.

23) Clark HF, Gurney AL, Abaya E, Baker K, Baldwin D, Brush J, Chen J, Chow B, Chui C, Crowley C, Currell B, Deuel B, Dowd P, Eaton D, Foster J, Grimaldi C, Gu Q, Hass PE, Heldens S, Huang A, Kim HS, Klimowski L, Jin Y, Johnson S, Lee J, Lewis L, Liao D, Mark M, Robbie E, Sanchez C, Schoenfeld J, Seshagiri S, Simmons L, Singh J, Smith V, Stinson J, Vagts A, Vandlen R, Watanabe C, Wieand D, Woods K, Xie MH, Yansura D, Yi S, Yu G, Yuan J, Zhang M, Zhang Z, Goddard A, Wood WI, Godowski P, Gray A. (2003) The secreted protein discovery initiative (SPDI), a large-scale effort to identify novel human secreted and transmembrane proteins: a bioinformatics assessment. Genome Res. Oct;13(10):2265-70. NCBI Reference Sequence: NM_198510.2

24) Midgley, A. C., Rogers, M., Hallett, M. B., Clayton, A., Bowen, T., Phillips, A. O. & Steadman, R. (2013). Transforming growth factor-beta1 (TGF-beta1)-stimulated fibroblast to myofibroblast differentiation is mediated by hyaluronan (HA)-facilitated epidermal growth factor receptor (EGFR) and CD44 co-localization in lipid rafts. J Biol Chem, 288, 14824-14838.

25) Bommaya G, Meran S, Krupa A, Phillips AO, Steadman R. (2011) Tumour necrosis factor-stimulated gene (TSG)-6 controls epithelial-mesenchymal transition of proximal tubular epithelial cells. Int J Biochem Cell Biol. 43(12):1739-46.

26) Webber, J., Meran, S., Phillips, A. & Steadman, R. (2009). Hyaluronan orchestrates TGF{beta}1-Dependent maintenance of Myofibroblast Phenotype. J Biol Chem, 284, 9083-9092

27) Lesley, J., English, N. M., Gal, I., Mikecz, K., Day, A. J. & Hyman, R. (2002). Hyaluronan binding properties of a CD44 chimera containing the link module of TSG-6. The Journal of Biological Chemistry, 277, 26600-26608.

28) Ochsner, S. A., Day, A. J., Rugg, M. S., Breyer, R. M., Gomer, R. H. & Richards, J. S. (2003). Disrupted function of tumor necrosis factor-alpha-stimulated gene 6 blocks cumulus cell-oocyte complex expansion. Endocrinology, 144, 4376-4384.

29) Jiang, D., Liang, J.,. & Noble, P. W. (2011). Hyaluronan as an immune regulator in human diseases. Physiol. Rev. 91 (1): 221-264.

30) Lewis, A., Steadman, R., Manley, P., Craig, K., de la Motte, C. A., Hascall, V. C. & Phillips, A. O. (2007). Diabetic nephropathy, inflammation, hyaluronan and interstitial fibrosis. Histology and Histopathology, In Press.

31) Banerji S, Wright AJ, Noble M, Mahoney DJ, Campbell ID, Day AJ, Jackson DG. (2007) Structures of the Cd44-hyaluronan complex provide insight into a fundamental carbohydrate-protein interaction. Nat Struct Mol Biol. Mar;14(3):234-9.

32) Day, A. J. & de la Motte, C. A. (2005). Hyaluronan cross-linking: a protective mechanism in inflammation? Trends Immunol, 26, 637-643.

33) Evanko SP, Tammi MI, Tammi RH, Wight TN. (2007) Hyaluronan-dependent pericellular matrix. Adv Drug Deliv Rev. Nov 10;59(13):1351-65.

34) Knudson, W., Aguiar, D. J., Hua, Q. & Knudson, C. B. (1996). CD-44 anchored hyaluronan-rich pericellular matrices: An ultrastructural and biochemical analysis. Experimental Cell Research, 228, 216-228.

35) Selbi W, de la Motte CA, Hascall VC, Day AJ, Bowen T, Phillips AO. (2006b) Characterization of hyaluronan cable structure and function in renal proximal tubular epithelial cells. Kidney Int. Oct;70(7):1287-95.

36) Selbi W, de la Motte C, Hascall V, Phillips A. (2004) BMP-7 modulates hyaluronan-mediated proximal tubular cell-monocyte interaction. J Am Soc Nephrol. 15(5):1199-211.

37) Sato, H., Kajikawa, S., Kuroda, S., Horisawa, Y., Nakamura, N., Kaga, N., Kakinuma, C., Kato, K., Morishita, H., Niwa, H. & Miyazaki, J. (2001). Impaired fertility in female mice lacking urinary trypsin inhibitor. Biochem Biophys Res Commun, 281, 1154-1160.

38) Zhuo, L., Yoneda, M., Zhao, M., Yingsung, W., Yoshida, N., Kitagawa, Y., Kawamura, K., Suzuki, T. & Kimata, K. (2001). Defect in SHAP-hyaluronan complex causes severe female infertility. A study by inactivation of the bikunin gene in mice. The Journal of Biological Chemistry, 276, 7693-7696.

39) Lesley, J., Gal, I., Mahoney, D. J., Cordell, M. R., Rugg, M. S., Hyman, R., Day, A. J. & Mikecz, K. (2004). TSG-6 modulates the interaction between hyaluronan and cell surface CD44. The Journal of Biological Chemistry, 279, 25745-25754.

40) Hamm A, Veeck J, Bektas N, Wild PJ, Hartmann A, Heindrichs U, Kristiansen G, Werbowetski-Ogilvie T, Del Maestro R, Knuechel R, Dahl E. Frequent expression loss of Inter-alpha-trypsin inhibitor heavy chain (ITIH) genes in multiple human solid tumors: a systematic expression analysis. (2008) BMC Cancer. 28;8:25. doi: 10.1186/1471-2407-8-25.

41) Veeck J, Chorovicer M, Naami A, Breuer E, Zafrakas M, Bektas N, Dürst M, Kristiansen G, Wild PJ, Hartmann A, Knuechel R, Dahl E. (2008) The extracellular matrix protein ITIH5 is a novel prognostic marker in invasive node-negative breast cancer and its aberrant expression is caused by promoter hypermethylation. Oncogene. 31;27(6):865-76.

42) Rose M, Gaisa NT, Antony P, Fiedler D, Heidenreich A, Otto W, Denzinger S, Bertz S, Hartmann A, Karl A, Knüchel R, Dahl E. (2014) Epigenetic inactivation of ITIH5 promotes bladder cancer progression and predicts early relapse of pT1 high-grade urothelial tumours.**Carcinogenesis.**;35(3):727-36.

43) Huth S, Heise R, Vetter-Kauczok C, Skazik C, Marquardt Y, Czaja K, Knuche R, Merk H, Dahl E and Baron J . (2015.) Inter-a-inhibitor heavy chain 5 (ITIH5) is overexpressed in inflammatory skin diseases and affects epidermal morphology in constitutive knockout mice and murine 3D skin models. Experimental Dermatology 24 (9): 663-668.

LEGENDS

Figure 1

The sequences of all six of the IαI heavy chains were obtained from Genebank and aligned using MegAlign software. The sequences of the putative binding sites of the heavy chains to chondroitin sulphate to form IαI are highlighted in the blue box. It can be seen that the sequence of HC4 is uniquely distinct from the other heavy chains at this site.

Figure 2

Human lung fibroblasts were growth arrested and were then stimulated with TGF-β1 (10 ng/ml). The RNA was collected at the times shown and the RQ of alpha sma, FnEDA, Bikunin (Bik) and TSG-6 were determined by RTqPCR. Data shown are the mean ± SEM of five independent experiments, each of which generated a mean of 3 replicates. * $p<0.05$, ** $p<0.005$ compared to 0 hrs.

Figure 3

Human lung fibroblasts were growth arrested and were then stimulated with TGF-β1 (10 ng/ml). The RNA was collected after 72h treatment and the RQ of alpha sma (B,D,F), and TSG-6 (C,E,G) were determined by RTqPCR. The panels show cells (A) treated with siCD44, lysed and protein extracted for CD44 Western Blot; (B) and (C) si-CD44. (D) and (E) EFGR inhibitor AG 1478 (10 μM). (F) and (G) ERK inhibitor PD98059 (10 μM). Inhibitors were added 4 h prior to TGFβ1 stimulation. Data shown are the mean and scatter of values in three independent experiments, each with between 2 and 3 replicates, except (D) and (E)- 1 experiment with 3 replicates. * $p<0.05$, ** $p<0.005$ compared to TGF-β1 treatment alone.

Figure 4

Confluent fibroblasts were growth-arrested in serum-free medium for 48 hours, then treated with either scrambled siRNA or siRNA specific for Smad 2 or Smad 3 as detailed in Methods. The cells were then incubated with TGF-β1 at 10 ng/ml in serum-free medium for 72 hours. Control cells remained in serum-free conditions, without TGFβ1. The cells were lysed, RNA extracted and RTqPCR for (A) alpha-sma or (B) TSG-6, carried out as described in Methods. Results are expressed as mean and scatter of values in two independent experiments, each with 2 or 3 replicates (*$p<0.05$, compared to Scrambled). Scrambled in (A) and (B) was independently analysed more frequently. (C) and (D) show the inhibition of SMAD2 and SMAD3 by siSMAD2 or siSMAD3 respectively in 3 independent experiments.

Figure 5

Human lung fibroblasts were growth arrested and were then stimulated with TGF-β1 (10 ng/ml). The RNA was collected after 72h treatment and the RQ of alpha sma (A,C,E,G), and TSG-6 (B,D,F,H) were determined by RTqPCR. The panels show cells treated 4 h before TGFβ1 stimulation with:- (A and B) si-Bikunin, (C and D) Cobalt Chloride (0.05 mM to 1 mM), (E and F) Oligo HA (at 50 μg/ml), (G and H) anti-TGS-6 antibody A38 and non-immune IgG control ((50 μg/ml). Data shown are the mean and scatter of values in three independent experiments, each with more than 2 replicates. * $p<0.05$, ** $p<0.005$ compared to scrambled (A and B) or TGFβ1-stimulated cells (C-H).

Figure 6

Human lung fibroblasts were growth arrested and were then either incubated with TGF-β1 (10 ng/ml) or serum-free medium alone in the presence (A38) or absence of anti-TSG-6 antibody A38 at 50 μg/ml. Cells were stained for EGFR (Ab GR01 1:30), visualised using AlexaFluor 488) and CD44 (Ab A020 1:200) (Merck Millipor), visualised with AlexaFluor 555). The images were merged to demonstrate the co-localisation of CD44 and EGFR (yellow). Nuclei were stained with DAPI and the central images show a 4 times magnification of sections of the images. Co-localization scatter plots were performed to confirm co-localization (depicted as *yellow areas*). Data shown are representative of three independent experiments.

Figure 7

A) The absolute copy number of each IαI heavy chain was determined by reading standard curves prepared by adding known numbers of molecules to the qPCR reaction. Heavy chain 5 was shown to be the predominant isoform. Results are mean ± SEM of 4 independent experiments.

B) Human lung fibroblasts were growth arrested and were then cultured in the presence or absence of TGF-β1 (10 ng/ml) for 72h. The cells were lysed with RIPA buffer and 30 μg of protein was separated on

7.5% polyacrylamide gels. GAPDH antibody was used as a loading control. Blots shown are representative of 4 experiments.

Top panel: Western blot showing that the amount of IaI heavy chain 5 present was markedly increased following stimulation with TGF-β1 Bottom Panel: Following TGF-β1 incubation the cells were treated with 10 μg/ml trypsin in PBS for 10 min at room temperature as previously shown to remove any cell surface/CD44-associated HA (43).

C) Cells were incubated with or without TGF-β1 (10 ng/ml) for 72h. The cells were then either left untreated or exposed to Streptomyces hyaluronidase (0.4 U in 400 μl PBS for 2h). All cells were then fixed with 4% paraformaldehyde in PBS for 20 min and stained with anti-HC5 antibody followed by FITC conjugated anti rabbit IgG in order to demonstrate the presence of heavy chain 5 on the cell surface. Data shown are representative of three independent experiments.

Figure 8

Human lung fibroblasts were growth arrested and were then in the presence (+) or absence (-) of TGF-β1 (10 ng/ml) for 72h. (A) The culture supernatant was collected and concentrated using Micron centrifugal filter (Millipore) with a 3 kDa cut off. The equivalent of 1 ml of supernatant was then loaded into each well of a 7.5% polyacrylamide gel. Western blotting was carried out to demonstrate the presence of the native proteins and higher molecular weight complexes of TSG-6, Bikunin and Heavy Chain 5. (B) TGFβ1-treated cells were lysed and split into two identical samples of 30 μg. One half was treated with chondroitinase ABC (0.166 U/ml; Sigma-Aldrich) and both samples were incubated at 37 °C over night. The samples were then separated on a 7.5% polyacrylamide gel and Western blotting was carried out using anti-HC5 in order to demonstrate the degradation of the higher molecular weight complexes containing Heavy Chain 5. All blots in A and B are representative of 3 independent experiments.

Figure 9

Human lung fibroblasts were growth arrested and were then stimulated with TGF-β1 (10 ng/ml) or placed in serum-free medium only (Con) for 72h. The cells were then lysed (150 μl RIPA buffer per well of a six well plate), and 30 μg was separated on a 7.5% polyacrylamide gel. They were then subjected to Western blotting for HC5 with GAPDH used as a loading control. Blots shown are representative of 4 independent experiments.

A-D) Cells were cultured in the absence (-) or presence (+) of TGF-β1 (10 ng/ml) plus either Scrambled siRNA (scr), or target-specific siRNA: A) siTSG-6, B) siHC5, C) siHC2, D) siBikunin

E-I) Cells were cultured in the absence (Con) or presence of TGFβ1 (10 ng/ml) together with either E) oligosaccharides of HA, F) cobalt chloride (1 mM), G) mAb A38 (50 μg/ml), compared to non-immune IgG, or H) Streptomyces hyaluronidase (0.4 U in 400 μl PBS for 2h). siCD44 was also used as above to specifically knockdown CD44 compared to scrambled control (Fig I) as above (A-D).

Figure 10

Human lung fibroblasts were growth arrested and were then stimulated with TGF-β1 (10 ng/ml) in the presence or absence of SiHC5. The RNA was collected after 72h incubation and the effect of SiHC5 on copy number of heavy chain 5 (A) and the RQ of alpha sma (B), or TSG-6 (C) were determined by RTqPCR. Data shown are mean and scatter of values from three independent experiments. * $p<0.05$ ** $p<0.005$ for siHC5 compared to scrambled.

Figure 1

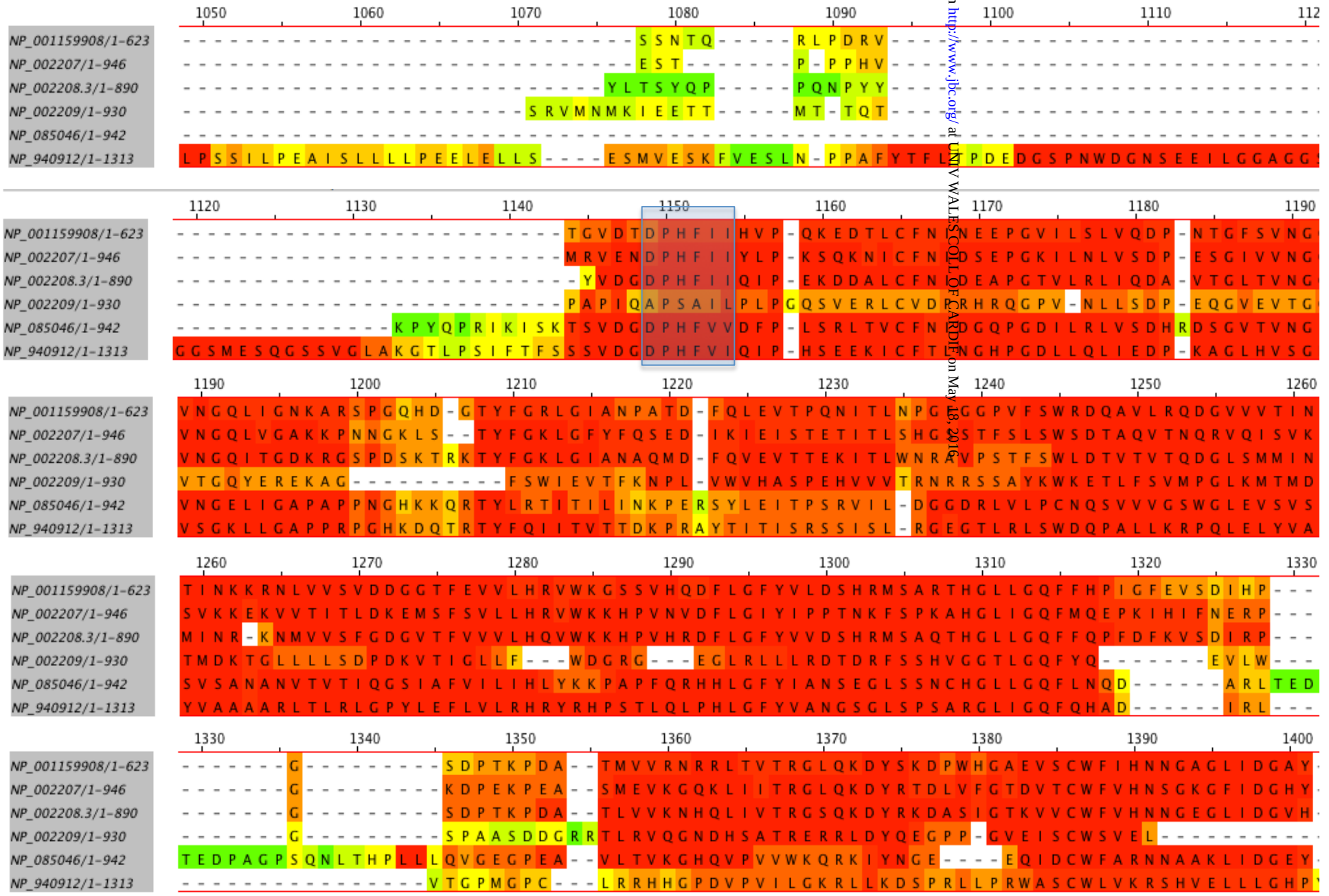

Figure 2

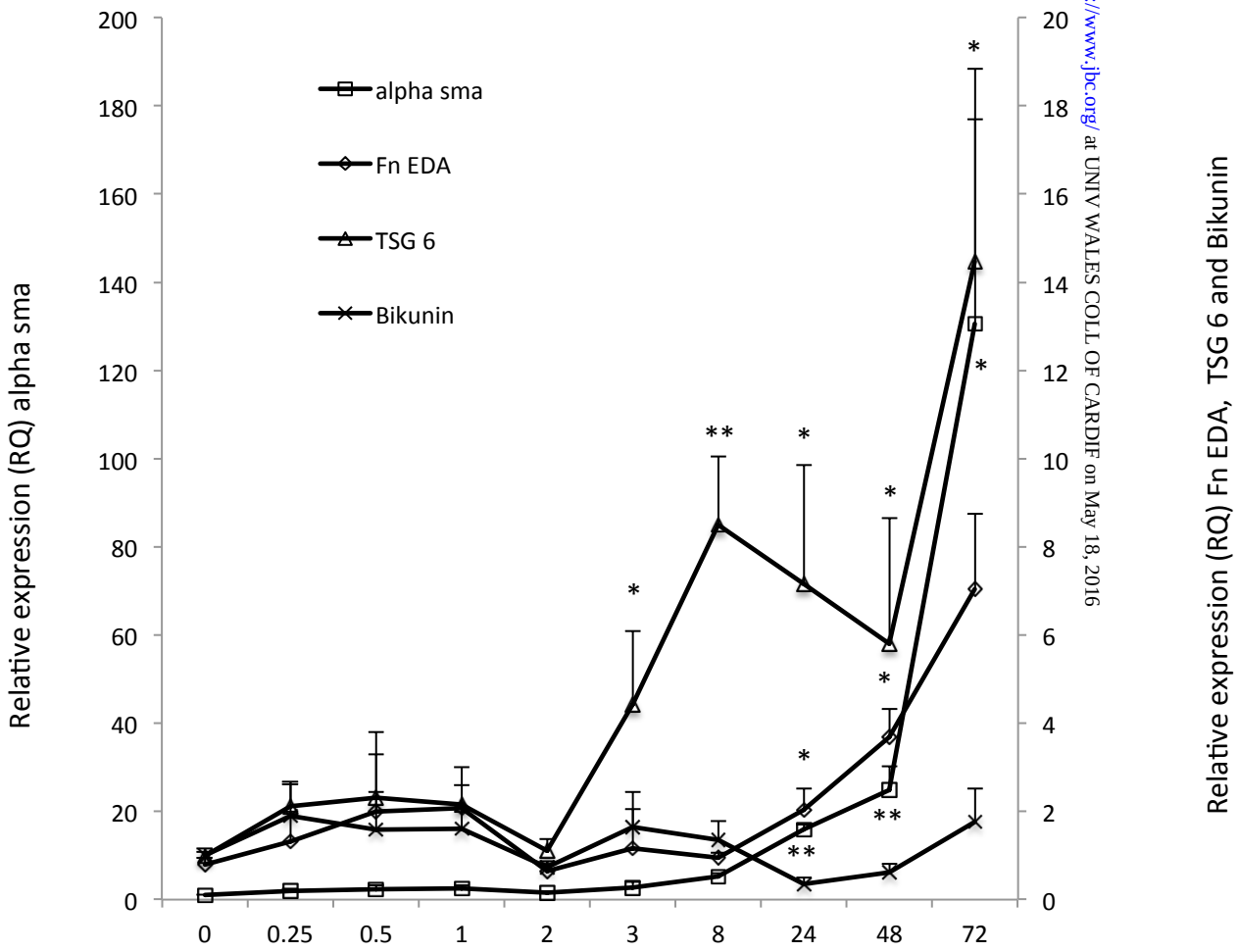

Figure 3

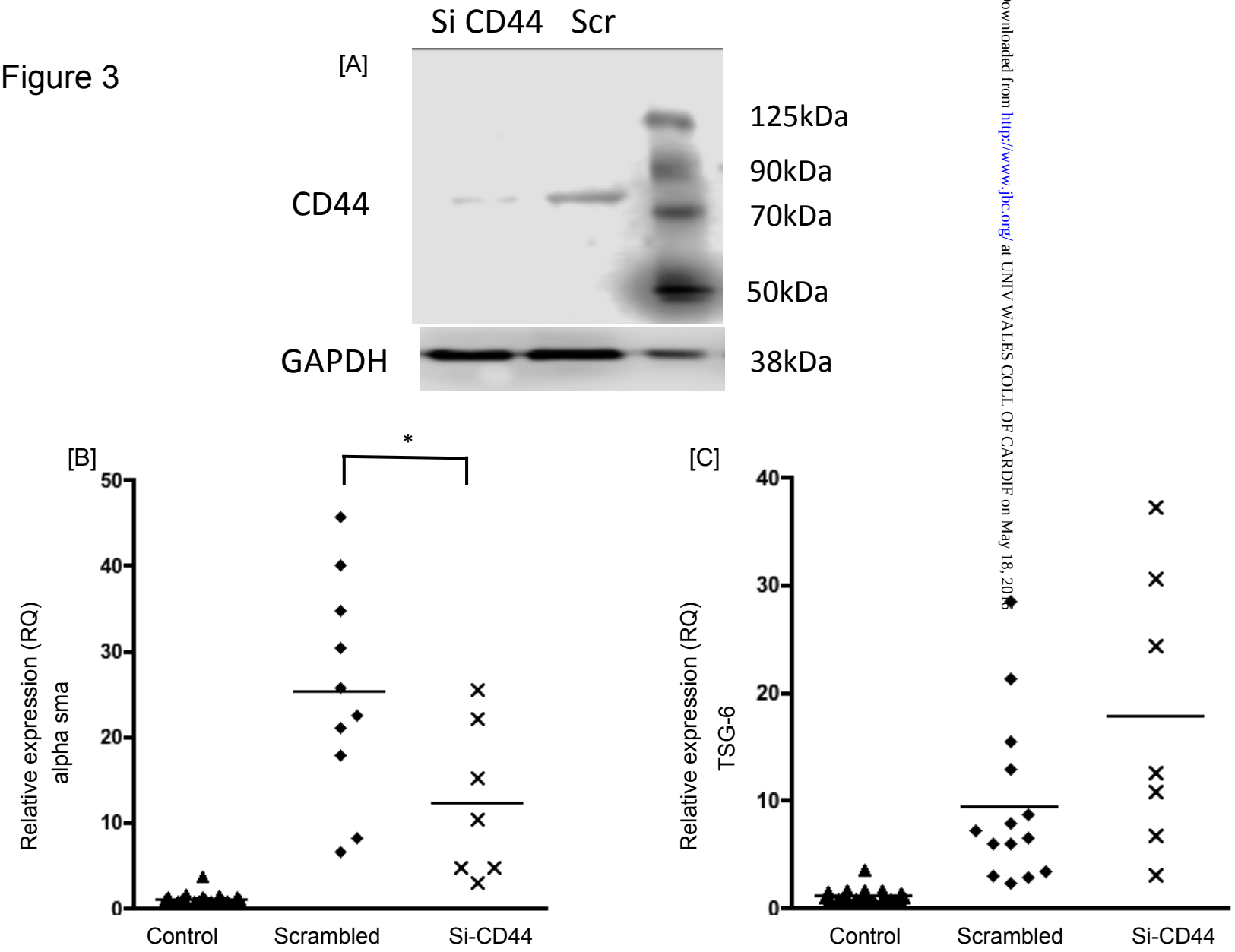

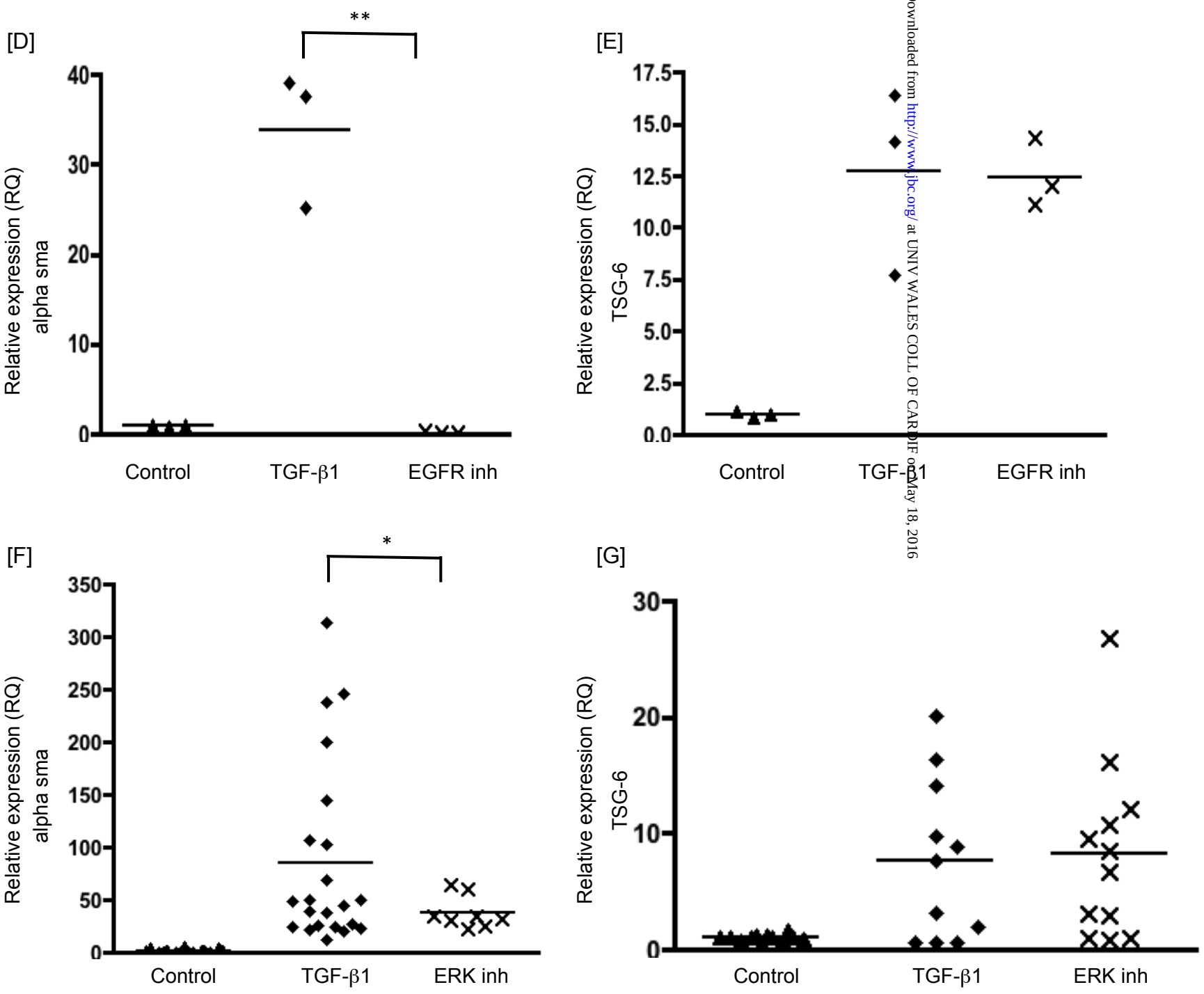

Figure 4

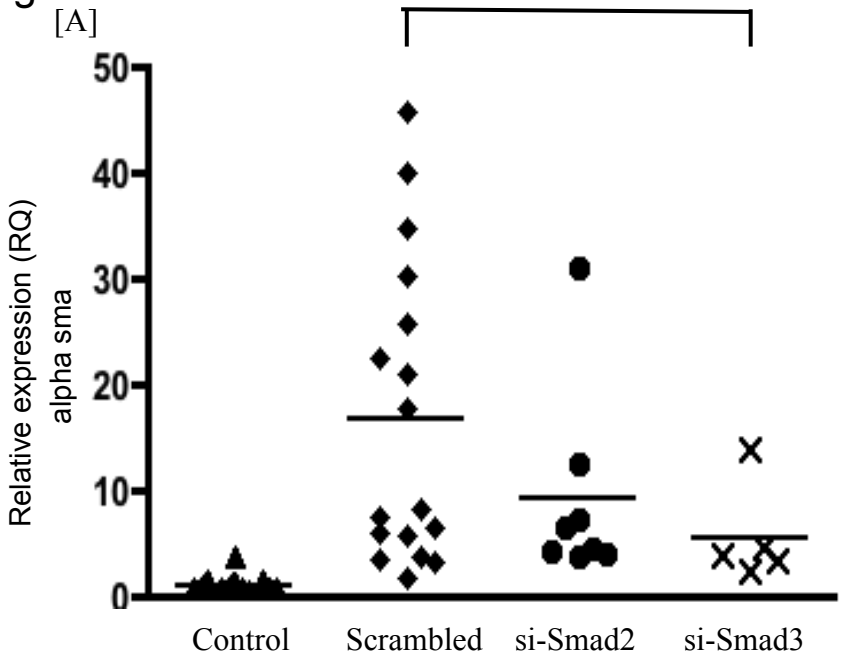

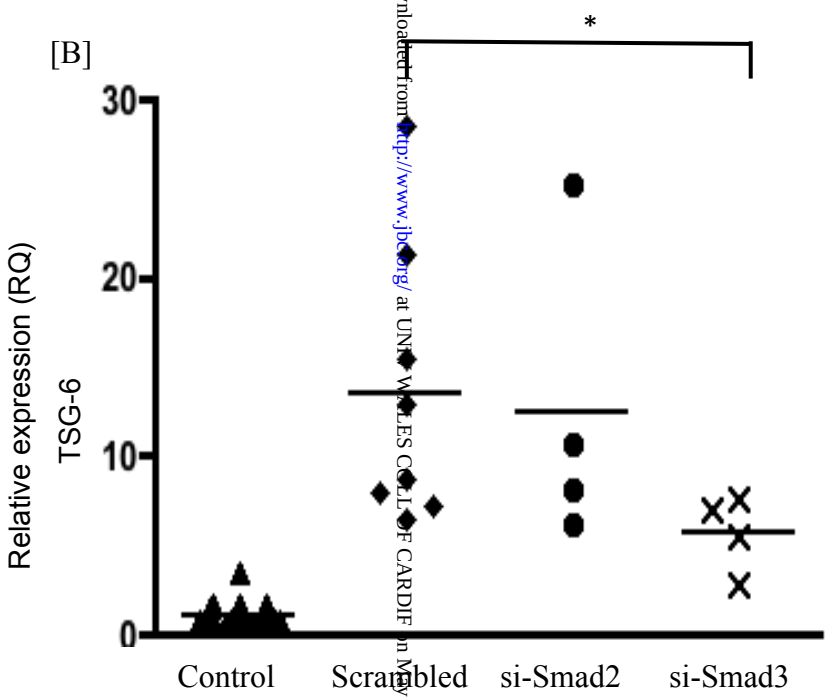

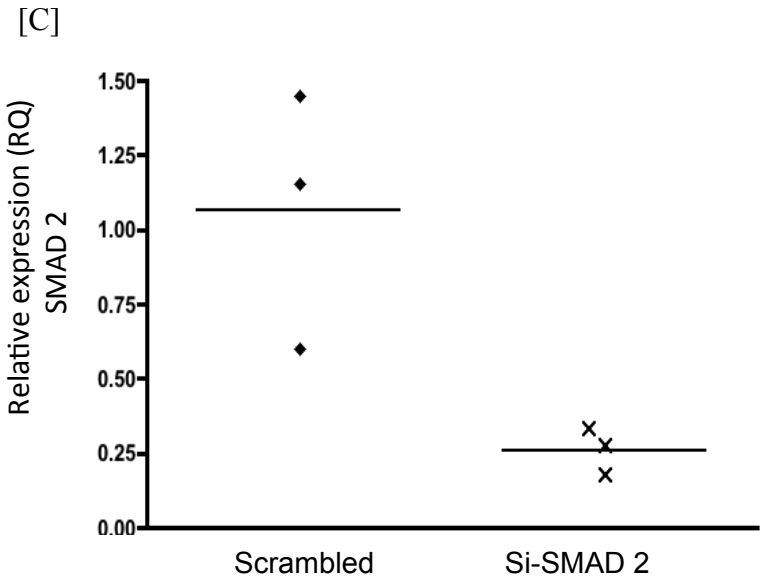

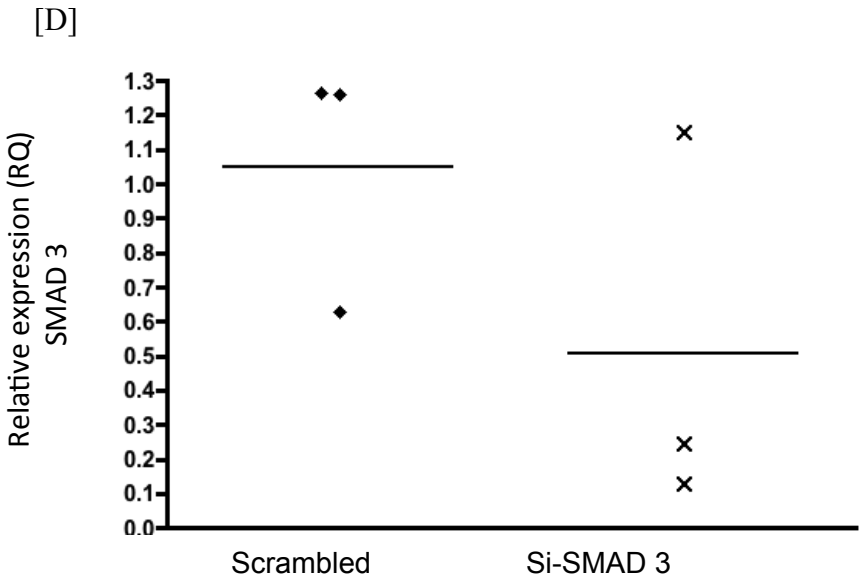

Figure 5

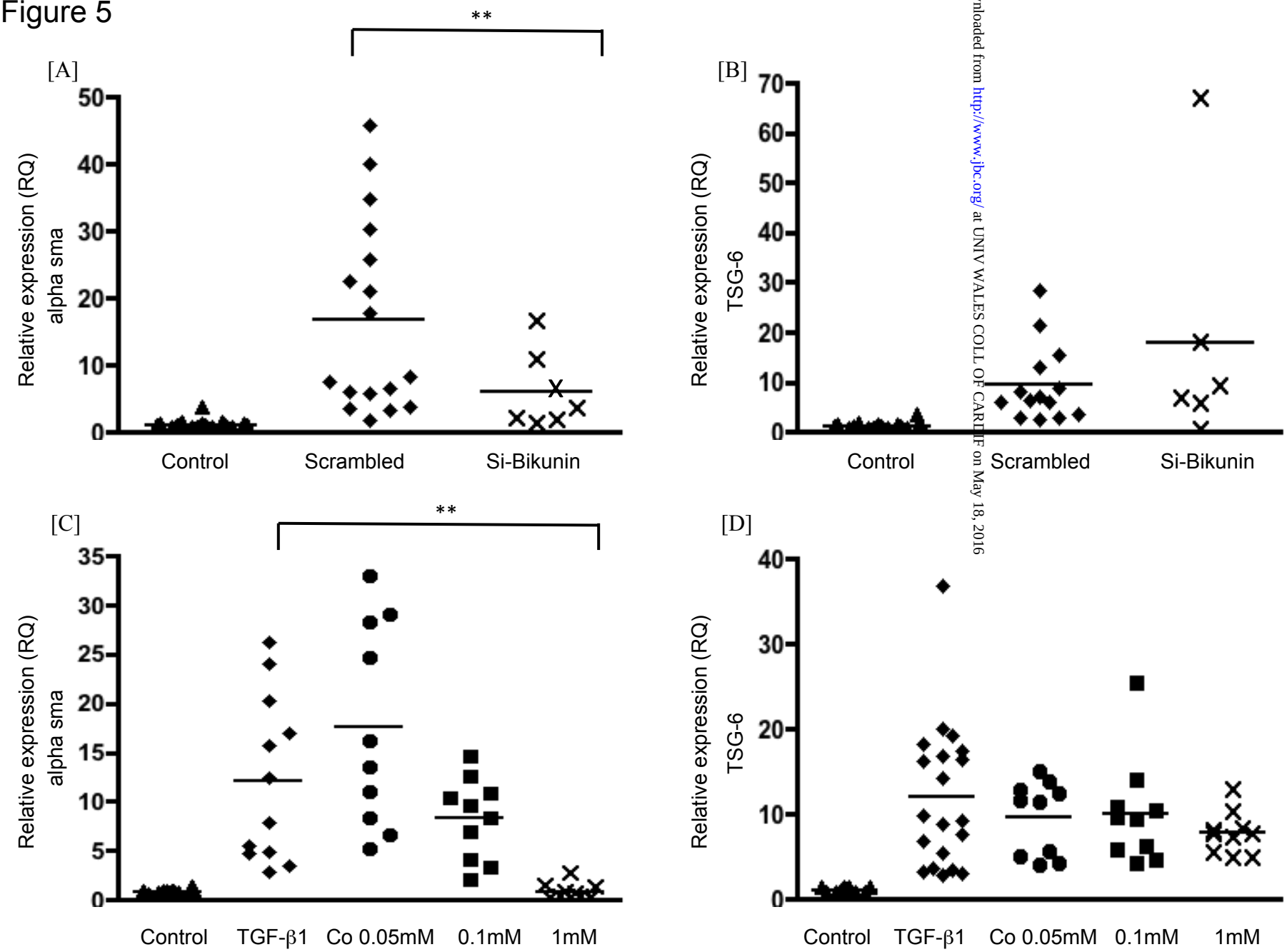

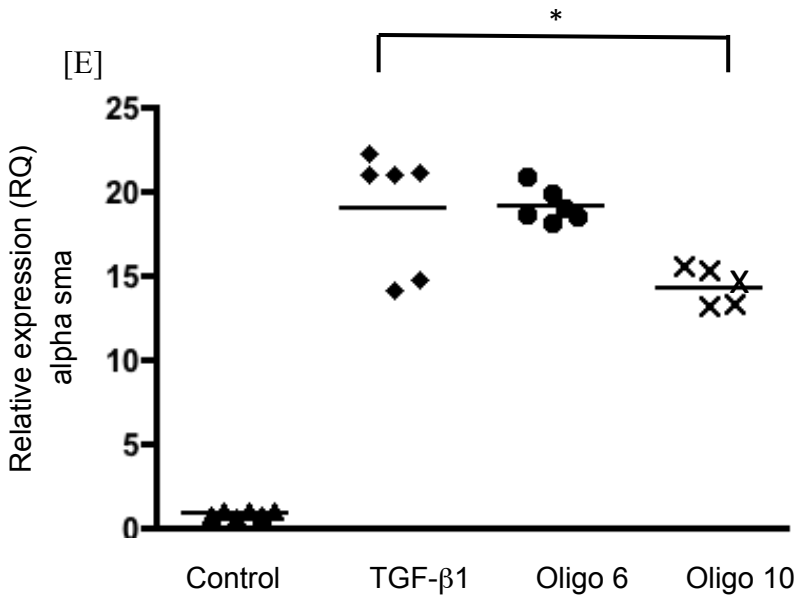

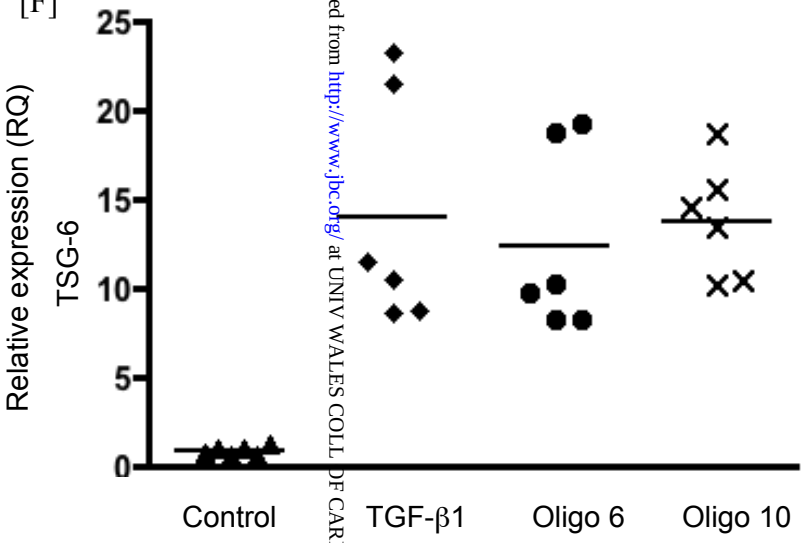

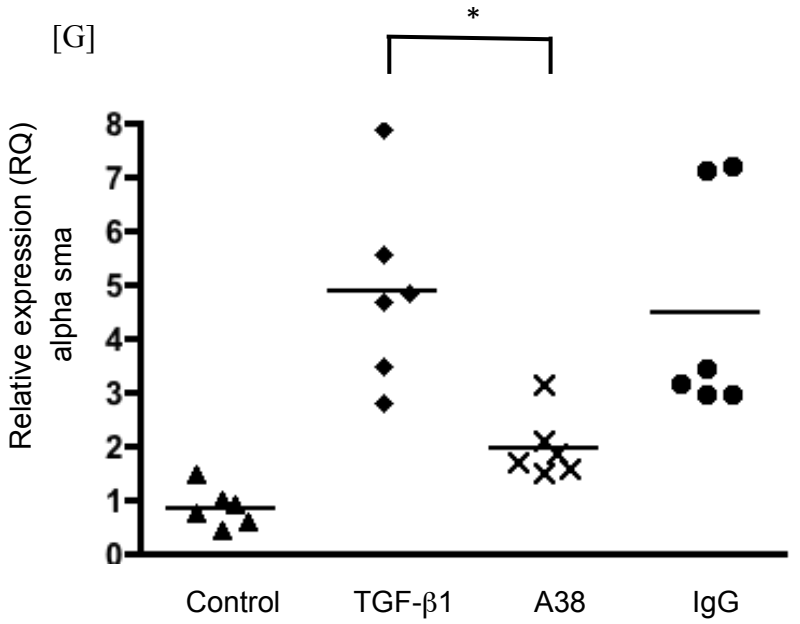

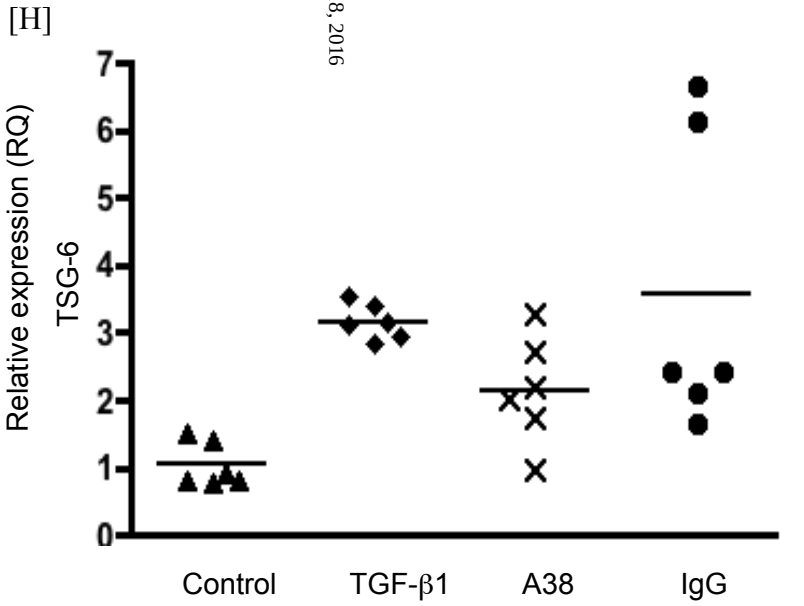

Figure 6

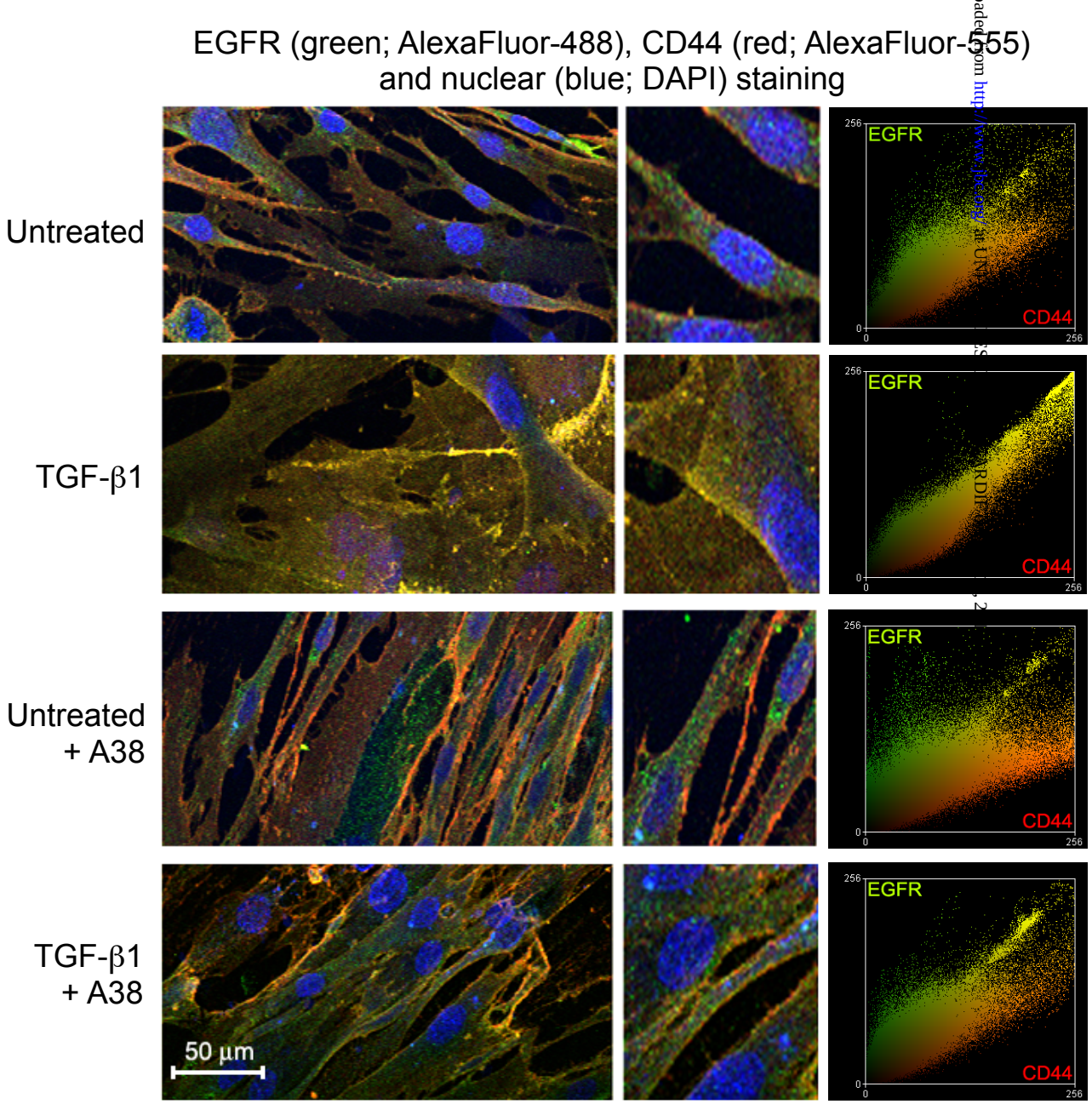

Figure 7

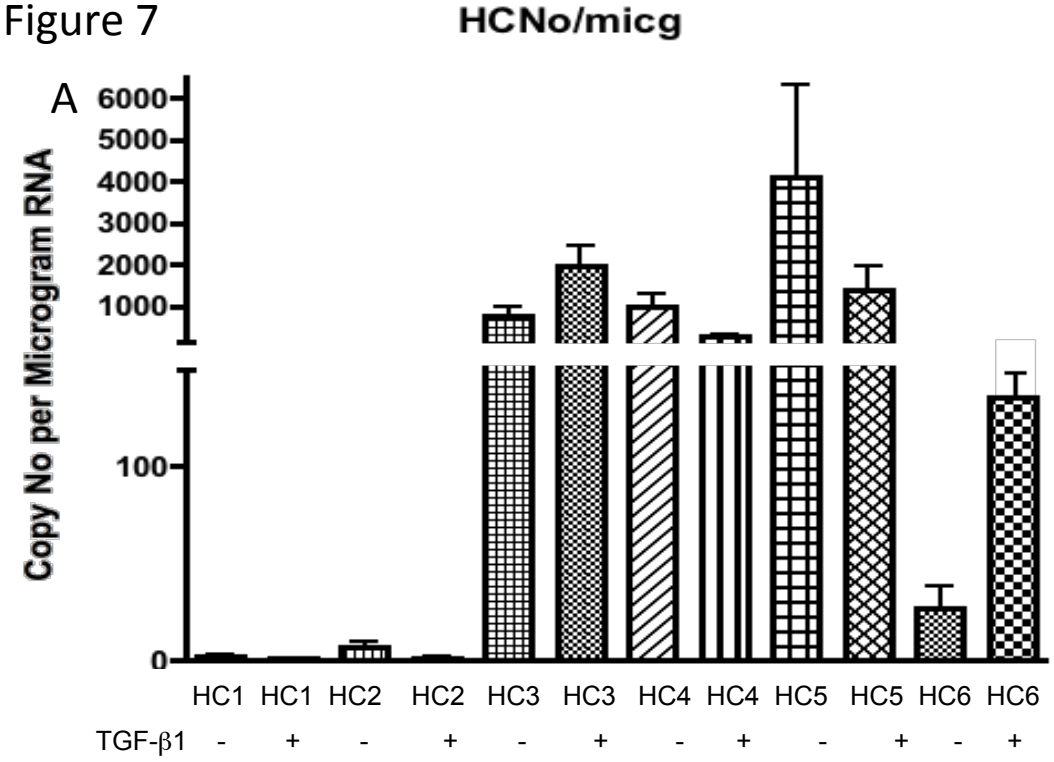

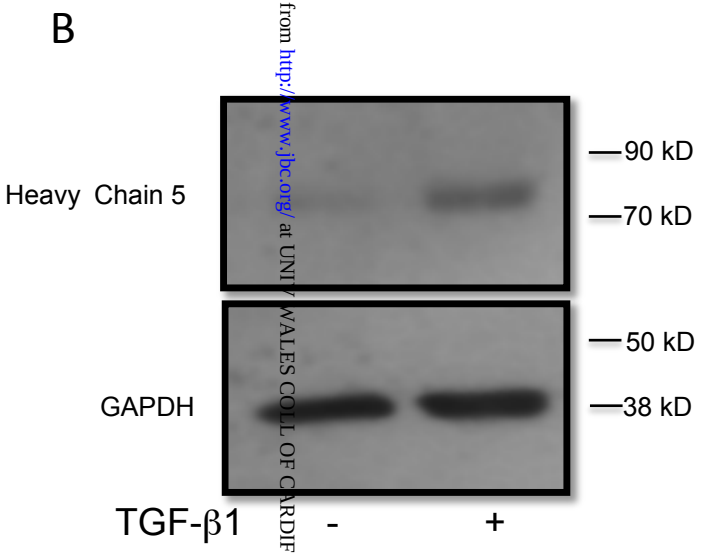

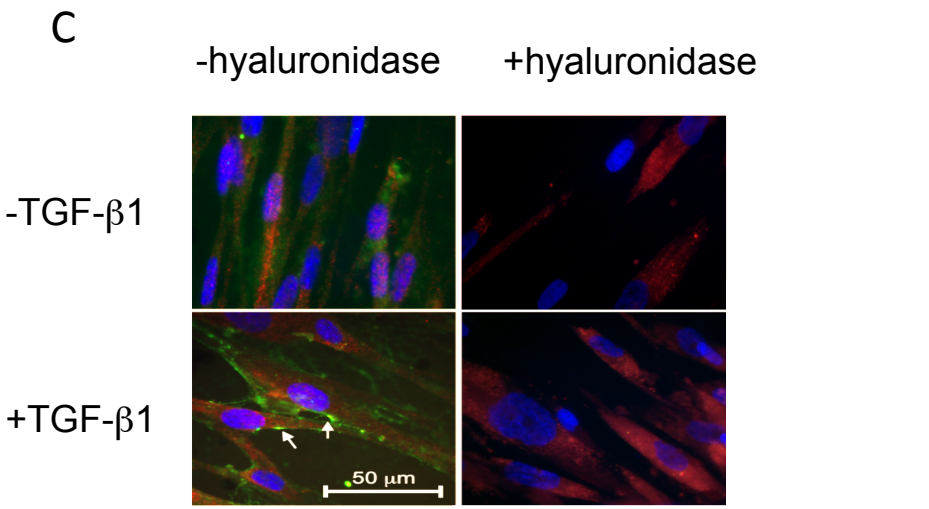

HA (green; AlexaFluor-488), HC5 (red; AlexaFluor-555) and nuclear (blue; DAPI) staining

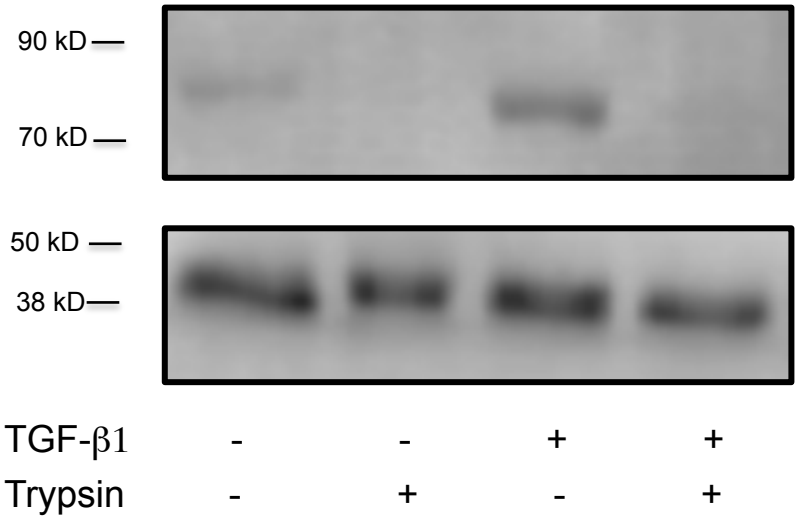

Figure 8

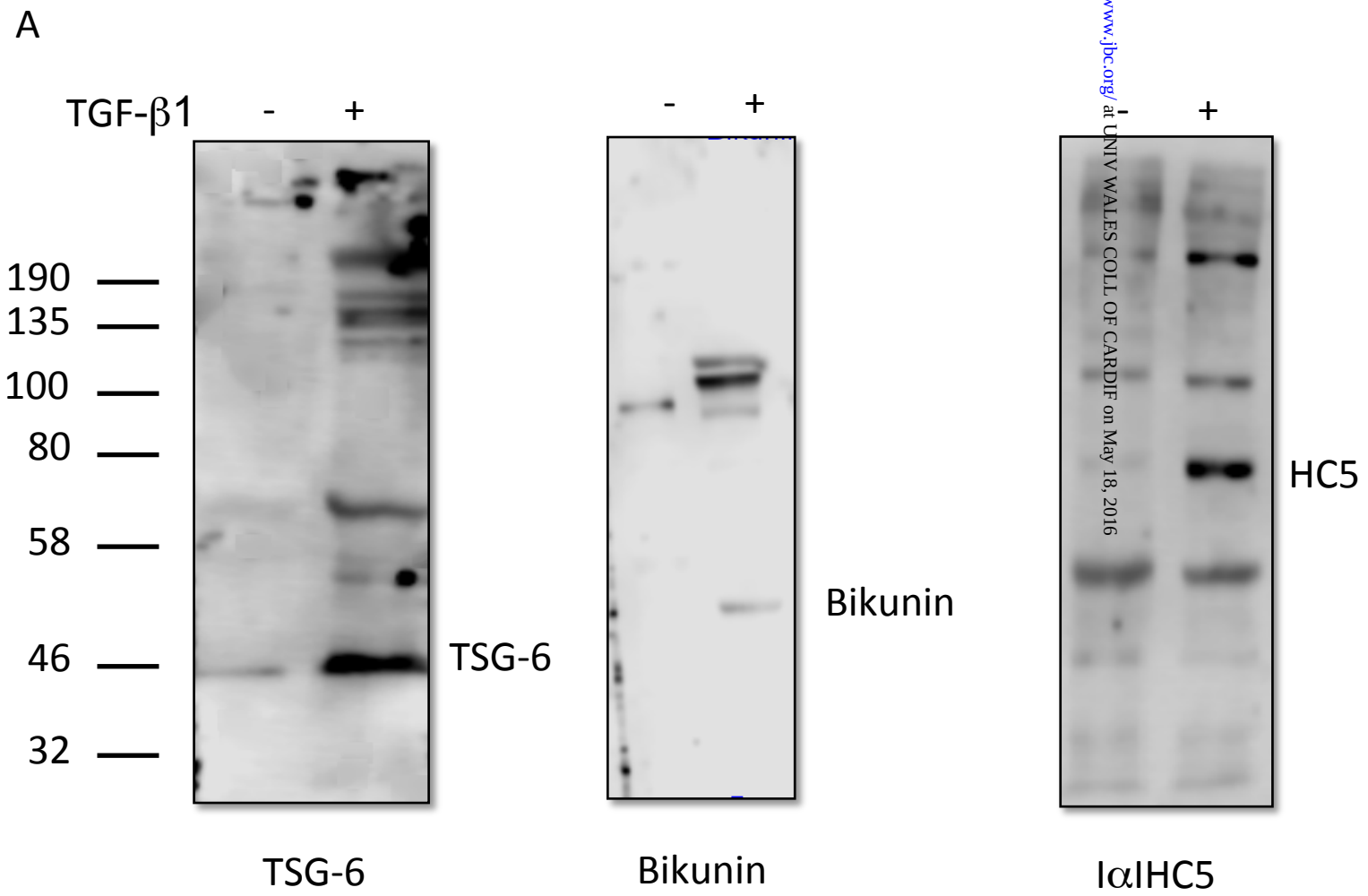

B

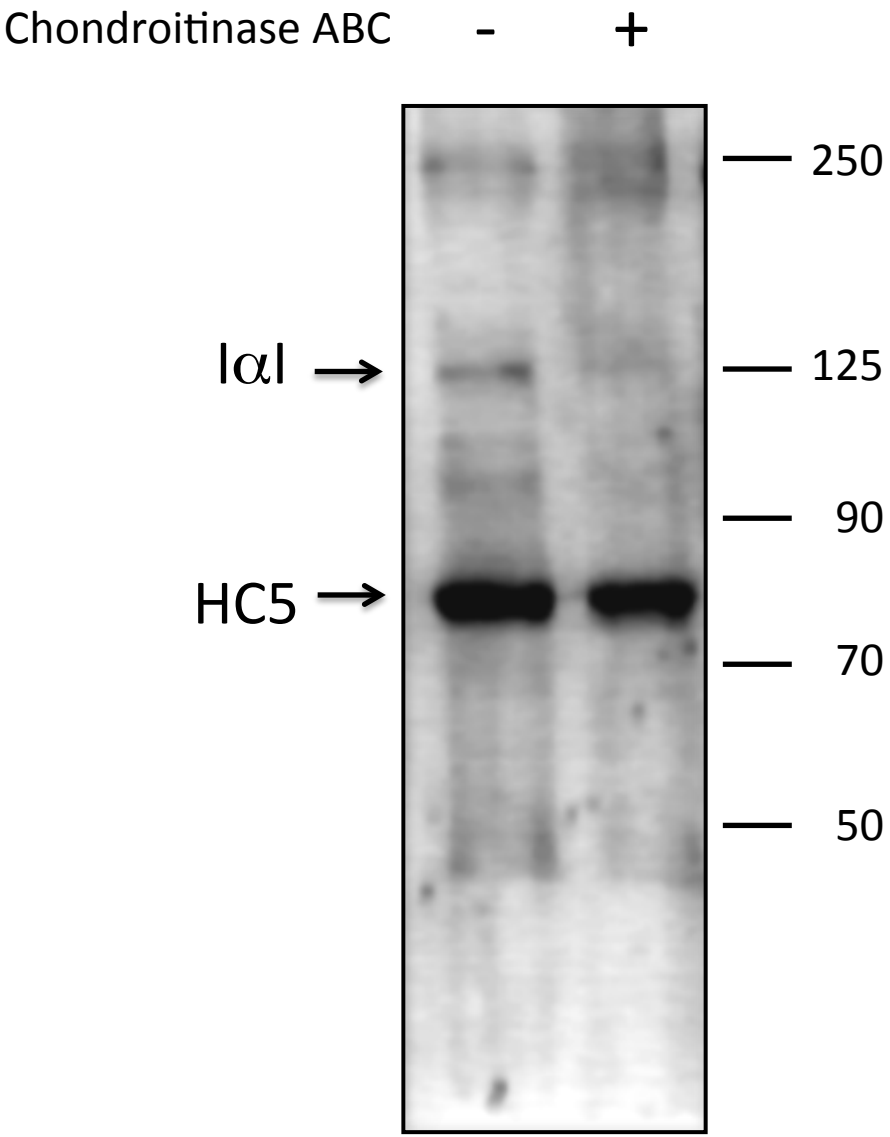

Figure 9

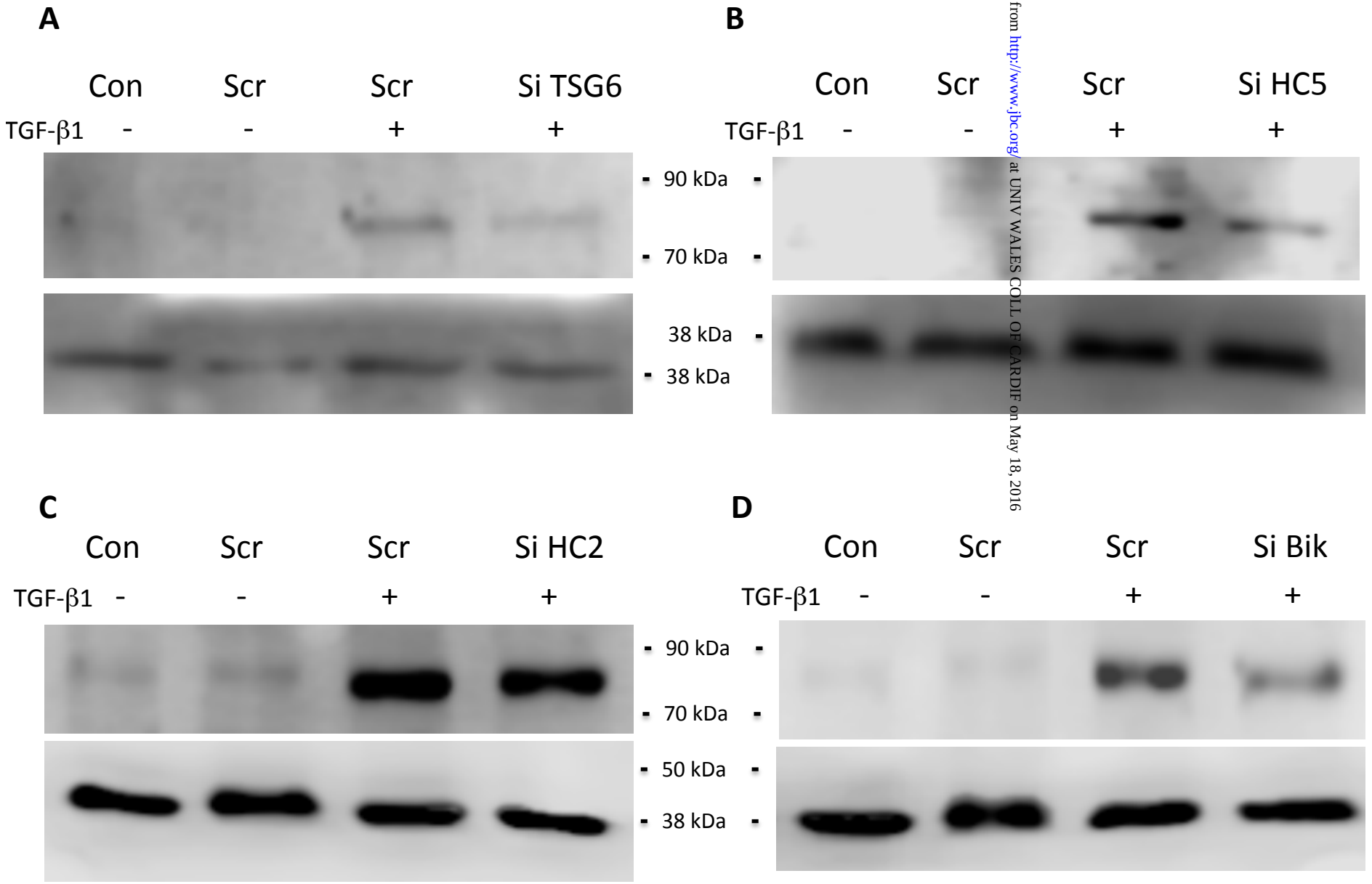

Figure 9

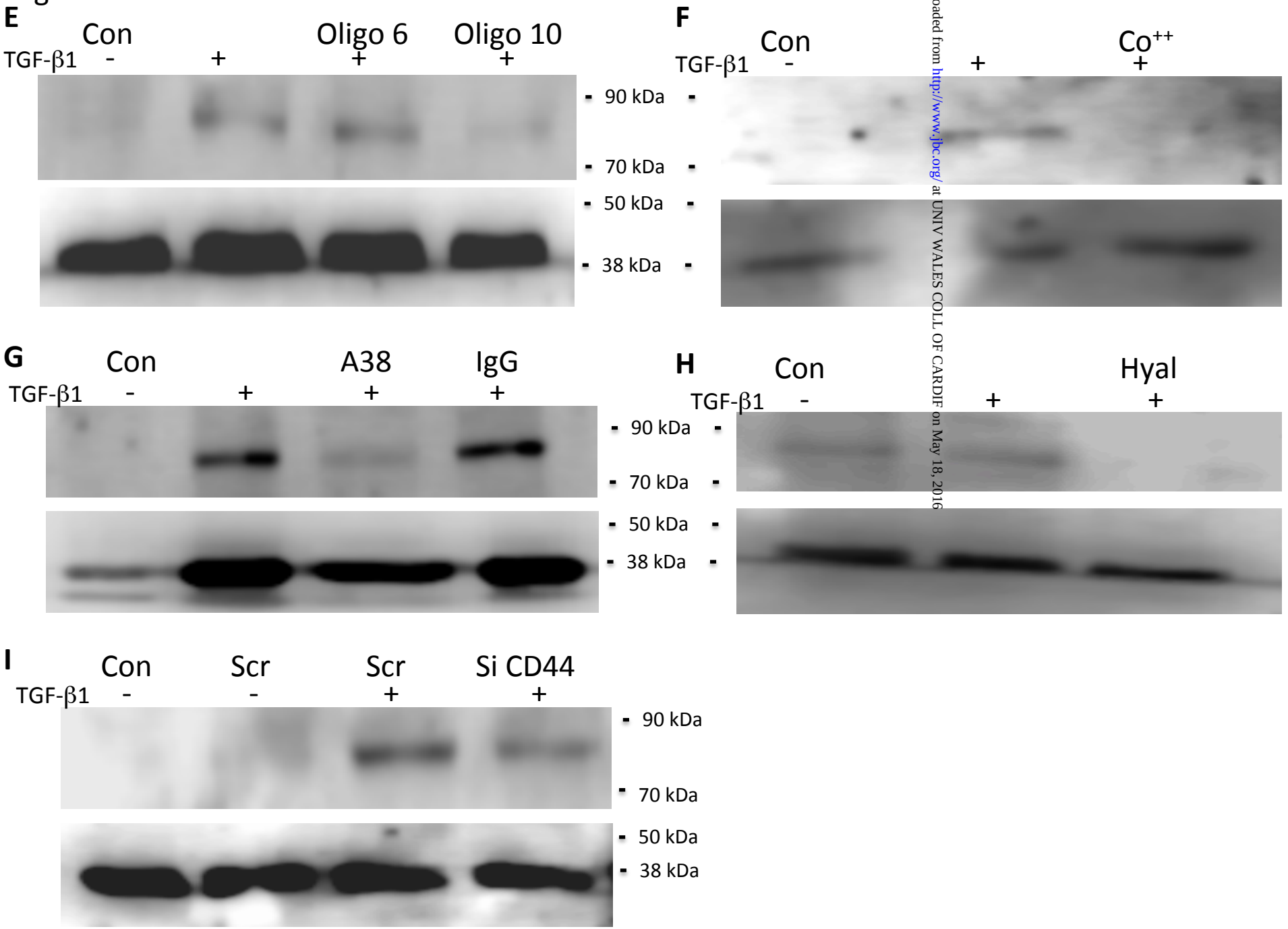

Figure 10

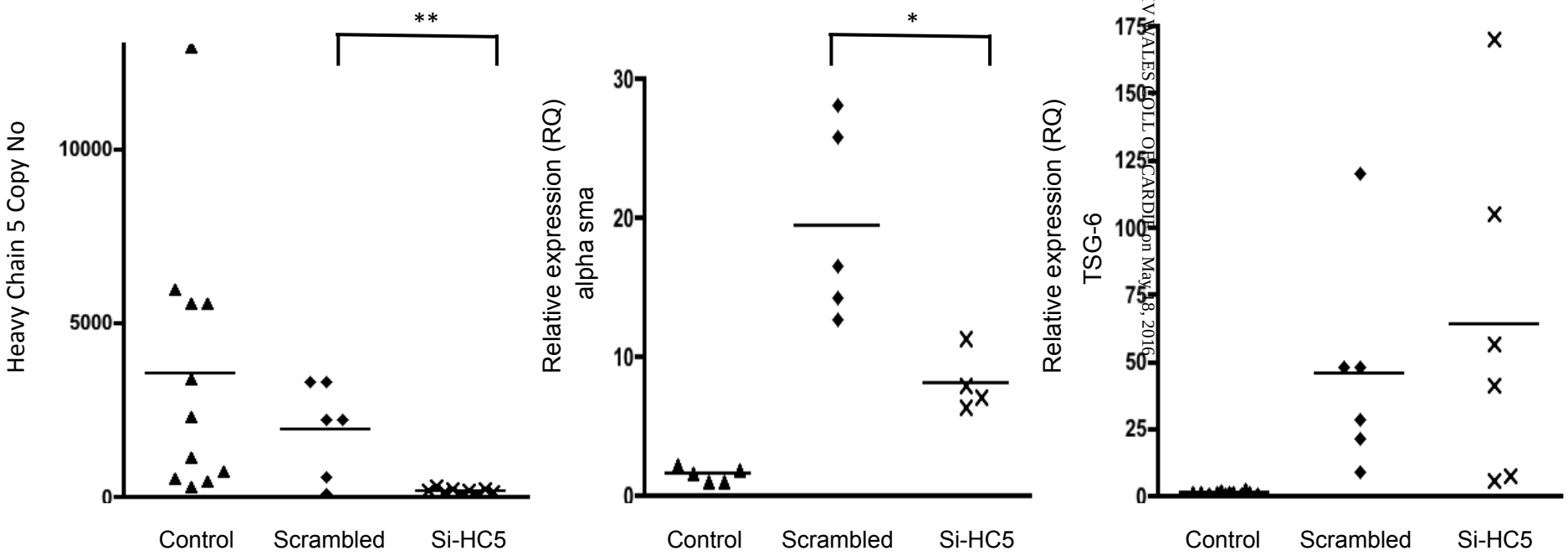

Tumour necrosis factor-stimulated gene (TSG)-6-mediated Interactions with the Inter-alpha-Inhibitor Heavy Chain 5 facilitate TGFbeta1-dependent Fibroblast to Myofibroblast Differentiation

John Martin, Adam Midgley, Soma Meran, Emma Woods, Timothy Bowen, Aled O. Phillips and Robert Steadman

J. Biol. Chem. published online May 3, 2016
